CONSTRUCTION OF LIGHT EMITTING NANOSTRUCTURES THROUGH SELF-ASSEMBLY OF OLIGOTHIOPHENE-BASED MACROMOLECULES FOR BIOMEDICAL APPLICATIONS

A THESIS SUBMITTED TO
THE GRADUATE SCHOOL OF ENGINEEERING AND SCIENCE
OF BILKENT UNIVERSITY
IN PARTIAL FULLFILMENT OF THE REQUIREMENTS
FOR
THE DEGREE OF
MASTER OF SCIENCE
IN
CHEMISTRY

By
Obadah Al Bahra

August 2016

Construction of Light Emitting Nanostructures Through Self-assembly of Oligothiophene-based Macromolecules for Biomedical Applications

By Obadah AL Bahra

August, 2016

We certify that we have read this thesis and that in our opinion it is fully adequate, in scope and in quality, as a thesis for the degree of Master of Science.

_____

Dönüş Tuncel (Advisor)

_____

Engin Umut Akkaya

_____

Salih Özçubukçu

Approved for the Graduate School of Engineering and Science:

_____

Levent Onural
Director of the Graduate School

ABSTRACT

Construction of light emitting nanostructures through self-assembly of oligothiophene-based macromolecules for biomedical applications

Obadah AL BAHRA

M.S. in Chemistry

Advisor: Dönüş TUNCEL

August 2016

This work discusses the synthesis and characterizations of oligothiophene-based macromolecules and the construction of nanostructures through self-assembly of these macromolecules in water. In order to prepare the macromolecules, first bi-functional oligothiophenes are synthesized, characterized and then, the properly functionalized polyethylene glycol is linked to oligothiophene through nucleophilic substitution reactions to obtain an amphiphilic macromolecule.

Self-assembly of amphiphilic macromolecules in water are investigated; the size and the morphology of the resulting nanostructures are determined by various techniques including dynamic light scattering, SEM and TEM. Their optical properties are studied using UV-vis and fluorescent spectroscopies.

Polyethylene oxide has been considered highly biocompatible and biodegradable material which make it candidate for the biological applications as carrier for bioactive materials and controlled releasing of the drugs.

Keywords: Oligothiophenes, polyethylene glycol, water soluble conjugated materials drug delivery

ÖZET

Oligotiyofen-temelli makromoleküllerin öz-eşleşmesi yoluyla biyomedikal uygulamalara yönelik ışık yayan nanoyapıların inşası

Obadah AL BAHRA

Kimya, Yüksek Lisans

Tez Danışmanı: Dönüş TUNCEL

Ağustos 2016

Bu çalışma oligotiyofen temelli makromoleküllerin sentez ve karakterizasyonunu, ve makromoleküllerin öz-eşleşme yoluyla nanoyapıların suda inşasını tartışmaktadır. Makromoleküllerin hazırlanması için ilk olarak iki fonksiyonlu oligotiyofenlerin sentezi, karakterizasyonu, ve sonrasında amfifilik bir makromolekül elde etmek için uygun olarak fonksiyonlandırılmış polietilen glikol oligotiyofene nükleofilik yer değiştirme reaksiyonuyla bağlanmıştır.

Amfifilik makromoleküllerin suda öz-eşleşmesi incelenmiştir; sonuçlanan nanoyapıların boyut ve morfolojileri, dinamik ışık saçılımı, SEM ve TEM içeren çeşitli yöntemlerle tayin edilmiştir. Bunların optik özellikleri UV-vis ve floresans spektroskopisi ile çalışıldı.

Polietilen oksit'in biyouyumluluğu yüksek ve biyoparçalanabilirliği dikkate alınmış malzeme olması, biyoaktif malzeme ve kontrollü ilaç salınımı için biyolojik uygulamalara taşıyıcı olarak aday olmanı sağlamaktadır.

Anahtar sözcükler: Oligotiyofenler, polietilen glikoller, suda çözünen konjuge malzemeler, ilaç iletimi.

Acknowledgment

I would like to thank my advisor Assoc. Prof. Dönüş Tuncel, for her guidance and supervision throughout the program. I would like also to thank the respected committee members, Prof. Engin U. Akkaya and Assist. Prof. Salih Özçubukçu, for their presence and taking the time to review and evaluate my thesis.

I am very grateful to former and present lab coworkers: Ahmet Koç and Sinem Gürbüz Şenol for their help and support, Canberk Uzundal, Dr. Maasommeh Bazzar who was always a great support and tea friend; special thanks to Hamidou Keita and Esra Deniz Soner for their amazing help, guidance on all aspects and accompanying me in long walks around the campus. An extra appreciation for Esra Deniz Soner for translating my abstract to Turkish. Also the friends from neighboring laboraotries, Dr. Vijaya Kumar, and all graduate neighbouring members. I also want to thank my lab friend Emre Koken not just for his friendship but also for sharing different kind of chemistry that we created in his kitchen.

I want to express my deepest appreciation to my dear cousin Mr. Muhanad and his wife Mrs. Özlem Younis for their incredible support from my very first step in Ankara Airport, for having me to their house with their lovely children and many beautiful memories.

The beautiful prayers and great wishes from mom, dad, brothers and all members of my big family who kept checking on me from everywhere. Their enormous faith in me is the only thing that made this work possible whenever I doubted it. The bless of having them very far, yet very close is priceless.

I wouldn't forget to thank my professors from Chemistry Department in Damascus University who introduced me to chemistry as its best.

I acknowledge whomever smiled and supported me for no reason but pure kindness coming out of their beautiful positive spirit Nimet Kaya Hanım from the graduate dorm management, Deniz Hanım and Emine Hanım from Chemistry Department, and all other sweet people I am proud to know.

I finally would like to express my gratitude giving credits to who really deserves it; Yurtdışı Türkler ve Akrabalar Başkanlığı for my scholarship and the opportunity for coming to Turkey and learn Turkish during the program, through the international Turkish scholarship (Türkiye Bursları).

I dedicate this work with all its great efforts

To the memory of my two best martyr friends

Mohammed and Ibrahim

and all innocent civil martyrs of Chemistry Department in Damascus University

to Syria ...

Contents

List of Figures

List of Tables

List of Schemes

Abbreviations

^{1}H-NMR	Proton-Nuclear Magnetic Resonance Spectroscopy
^{13}C-NMR	Carbon-Nuclear Magnetic Resonance Spectroscopy
LC-MS/TOF	Liquid Chromatography Mass Spectrum Time of Flight
UV-VIS	Ultraviolet-Visible Spectroscopy
FT-IR	Fourier Transform Infrared Spectroscopy
PL	Fluorescence Spectroscopy
DLS	Dynamic Light Scattering
SEM	Scanning Electron Microscope
TEM	Transmission Electron Microscope
TLC	Thin Layer Chromatography
$CDCl_3$	Deuterated chloroform
DCM	Dichloromethane
EtOAc	Ethyl acetate
DMF	Dimethyl formamide
DMSO	Dimethyl sulfoxide
DMSO(D_6)	Deuterated DMSO
THF	Tetrahydrofuran
D_2O	Deuterium oxide
TsCl	Tosyl Chloride
TPP	Triphenylphosphine
2TE	2-(thiophen-2-yl)ethanol
3TE	2-(thiophen-3-yl)ethanol

M1	2-(5-Bromo-2-thienyl)ethanol
M2	2-(5-Bromo-2-thienyl)ethyl 4-methylbenzenesulfonate
M3	2-(2-bromothiophen-3-yl)ethanol
TET1	2,2'-([2,2':5',2":5",2"'-quaterthiophene]-5,5"'-diyl)diethanol
TET2	2,2':5',2":5",2"'-quaterthiophene]-5,5"'-diylbis(ethane-2,1- diyl) bis(4-methylbenzenesulfonate
TET3	5,5"'-bis(2-azidoethyl)-2,2':5',2":5",2"'-quaterthiophene
dd water	Deionized water (18.2 ΩM)

Chapter 1

INTRODUCTION

1.1 Conjugated materials

1.1.1 Historical introduction

With rising the industrial revolution and the golden age of natural sciences starting in eighteenth century and flourishing in nineteenth century, the conjugated materials witnessed its first appearance about hundred fifty years ago in the mid nineteenth century by Henry Letheby in 1862 who obtained polyaniline from anodic oxidation of aniline, where he observed color changes on the product and electrochromic behavior. [1] However, the concept of macromolecules was not found before 1920s by the genuine work of Hermann Staudinger whom received Nobel Prize for his work 1953. [2] Soon after that, the first notable synthesis for a conjugated material was done by the famous Chemistry Nobel laureate 1963 Giulio Natta. [3- 4]

The real revolution in conductive polymers was made in 1970s by collaborative work of Alan G. MacDiarmid, Alan J. Heeger and H. Shirakawa, where polyacetylene was synthesized and studied thoroughly, [5] since then after the doors were widely opened for the investigation of the various properties and characteristics of conjugated materials leading to Nobel prize in 2000 in chemistry to the three professors MacDiarmid, Heeger and Shirakawa.

The most important structural feature in all conjugated materials (polymers and oligomers) is the alternating single strong head-head bonded orbitals, as localized σ bonding with double or triple weaker p-orbitals parallel π bonds [6] (Figure 1.1), this interaction of alternative single/ double bonds on a long chain forms the conjugated system (Figure 1.2).

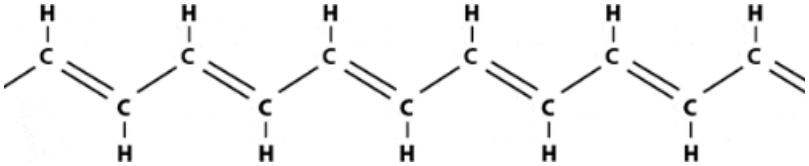

Figure 1.1 polyacetylene repeating units

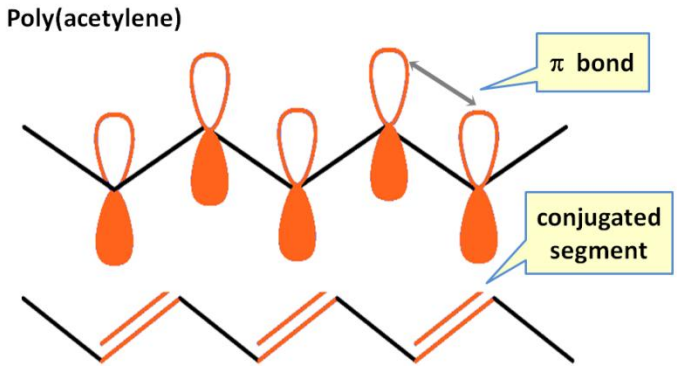

Figure 1.2 π conjugation

Conjugated materials are not limited to polyacetylene derivatives, it developed in many other complex conjugated systems, starting from simple aromatic cycles such as polyphenylenes to polymers depending on heterocyclic compounds such as polythiophene, polypyrrole; later on conjugated different co-polymers were introduced which give special property with every change in the units (Table 1.1).

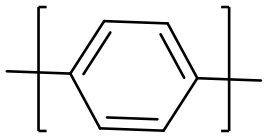	Poly(*p*-phenylene)
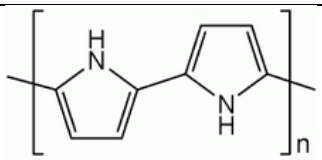	Polypyrrole
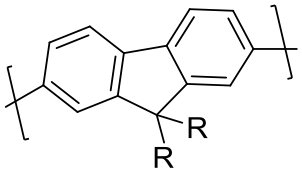	Polyflourene
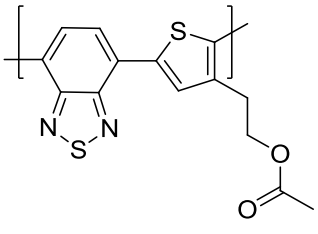	Poly [2-(2,5-dibromo-thiophen-3-yl)-ethyl acetate)-co-4,7-(2,1,3-benzothiadiazole)] Ref [7]

Table 1.1 Conjugated materials.

1.1.2 Structure and properties

The electronic properties of the conjugated materials are mostly determined by the π- electrons, which their distribution over the backbone effects the size of the band gap (Energy gap E_g) between the highest occupied molecular orbitals and lowest unoccupied molecular orbitals which are referred to as HOMO/ LUMO orbitals [8] respectively.

In term of conductivity, materials are classified in three categories, (1) Insulators: Materials that have wide band gap energy E_g> 6 eV, like many organic and polymers such as polystyrene, (2) Semiconductors: Materials with band gap energy which is around 1 eV, (3) Conductors: Materials that have overlapping between valence and conductive band which eliminates the band gap energy E_g= 0 eV like metals. [9] (Figure 1.3a,b).

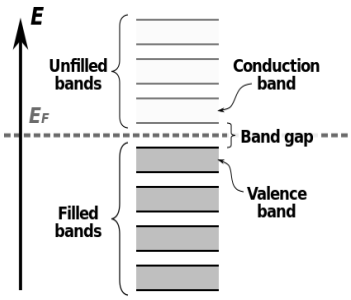

Figure 1.3a Electronic structure

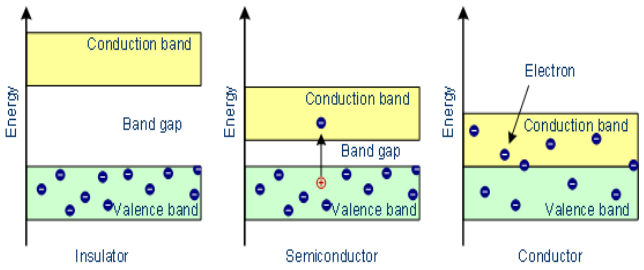

Figure 1.3b Materials' different types (right).

Increasing the conductivity can be achieved by decreasing the band gap which is called "doping" that can basically be done in two different methods forming either n-type semiconductors or p-type semiconductors. N-type semiconductors are produced by doping extra electrons to electronic orbitals. These electrons are going to be the charge transferring agents in N-type dopants, while P-type semiconductors are produced by removing electrons from the electronic orbitals

forming holes that will take place in charge transferring. Although both dopants are common, however, in organic semiconductors p-type is the more common as Hegger showed in his 1978 publication, polyacetylene p-type dopant is formed by oxidation which appears when films of the polymer are exposed to electron accepting vapors. [10]

Exposing conjugated material to light excites electrons in valence band to higher empty electronic orbitals in conductive band, this absorbed energy by the electrons is released in either radiative or non-radiative decay process. Non-radiative process includes activities like heat. The radiative decay process means that the energy is released as emitting light photon which its energy related to the band gap of the material, this process is called photoluminescence. [11] If the photon is released directly from the lowest LUMO singlet excited state then the process is fluorescence, the lifetime of fluorescence is very short (nanoseconds) so emission would disappear after removing the light source. If excited electron before returning to the ground state was subjected to intersystem crossing to triplet state then the photoluminescence activity is phosphorescence; phosphorescence has longer lifetime that might take several minutes. [11] Jablonski Diagram explains the photoluminescent phenomena (Figure 1.4).

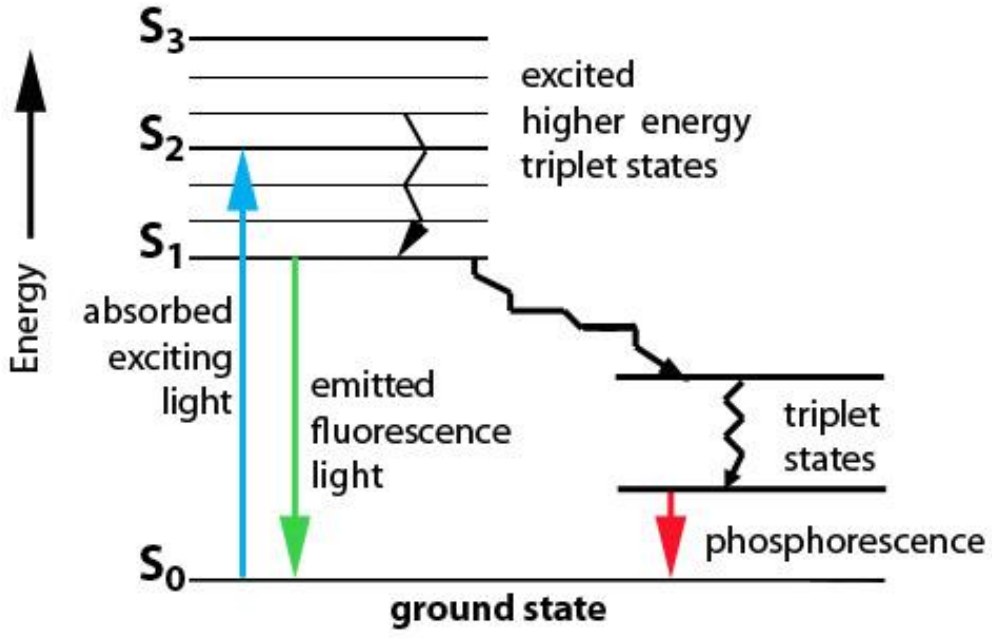

Figure 1.4 Simplified Jablonski Diagram.

1.1.3 Five-membered heterocycles

Most commonly when talking about Poly(heterocycles) and oligo-heterocycles, the main building block for five membered heterocycles are thiophene, furan and pyrrole. The first synthesized polymers upon these was poly(pyrrole). [12] As a simple definition the product is an extended conjugated system of polyacetylene stabilized by heteroatom. The advantage of the materials synthesized starting from the monomers mentioned above comes from the flexibility of modifying the monomer structure thus, modulating the electronic and electrochemical properties of the products. Additionally, comparing to polyacetylene they have non-degenerated ground state and they have higher environmental stability. [13]

Oxygen in furan has two lone pairs of electrons of which one of them contributes in the cycle making six delocalized π-electron planner, while the other stays unpaired 2p lone pair, however, the high electronegativity of oxygen atom makes it electron withdrawing, therefore, the positive trivalent oxygen makes the dipolar structures less stable which makes the aromatic character of furan less than the one in pyrrole and thiophene, where lower dipole moment makes higher aromatic character to the ring. This correspond to Pauling rule of electronegativity. [14, 15] (Table 1.2).

Molecule	Resonance Energy (kJ.mol^{-1})	Electronegativity
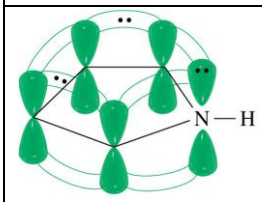 Pyrrole	100	3.0
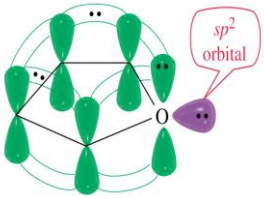 Furan	80	3.5
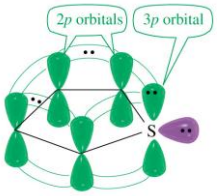 Thiophene	120	2.5
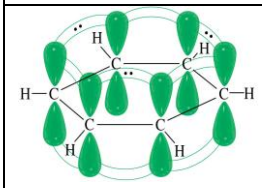 Benzene	150.2	

Table 1.2 Aromaticity differences in 5-membered heterocycles comparing to benzene. Ref [16].

Because of the aromatic character with heterocenter, these molecules differ in term of electrophilic reactivity; pyrrole> furan> thiophene> benzene. The electrophilic substitution is regioselective where it mostly occurs on 2,5 positions (α) rather than 3,4 (β) position, this is due to the relatively stable protonated intermediate of 2,5 substituted fractions. The substitution on 3,4 positions occurs after 2,5 are already substituted. [16] (Scheme 1.1).

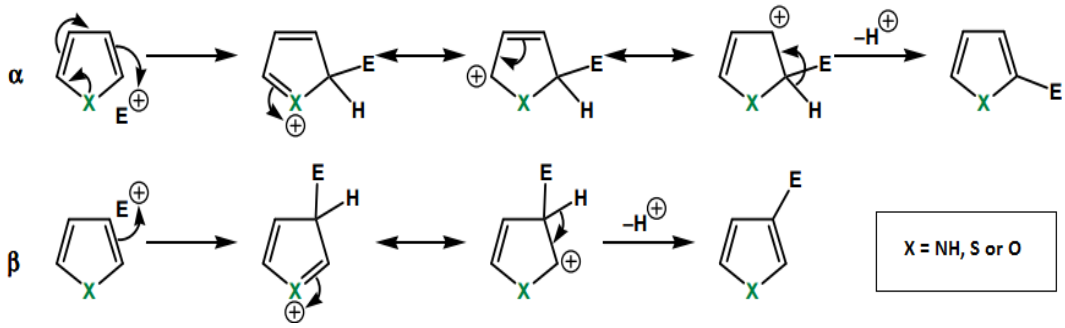

Scheme 1.1 Electrophilic substitution on 5-membered heterocycles.

1.1.4 Synthesis

The synthesis of conjugated materials falls in two main categories, the first part is functionalizing the monomeric building blocks, these reactions follow the traditional organic reactions (bromination, hydrolyzation, acetylation, esterification, etc), the other part is coupling the monomers together and forming carbon- carbon bond, in oligomeric or polymeric structures that is controlled by the precursors and their functionalities. The formed oligomers and polymers might be subjected to extra modifications relevant to increase properties and remove protecting groups.

The carbon carbon coupling reactions witnessed massive development, in mid-20th century it used to be done with methods like electrochemical (anodic, cathodic) polymerization with supporting electrolytes such as $KClO_4$, $NaClO_4$; [13,17, 18] oxidation with Friedl-Craft route; [13, 19] the metallic catalyzation into organic synthesis was firstly introduced by 1912 Nobel Chemistry Laurite Victor Gringard using metals like magnesium to form C-C bond, these organometallic compounds where used as intermediates in Pd/ Ni catalyzed condensation polymerization developed and published by Makoto Kumada in 1972. [20,21] In 1994 Katsutsugu Kitada and Shoichiro Ozaki reported Reductive Polymerization of Halothiophene, by palladium catalyzation only. The revolution in metal catalyzed reactions started in the seventies of twentieth century, flourished in last decade and finally crowned in 2010 by Nobel Prize in Chemistry awarded to Akira Suzuki, Richard F. Heck and Ei-ichi Negishi for their original

work on palladium catalyzed cross coupling since the 1970's. [22] John Kenneth Stille was also an important developer of famous palladium catalyzed cross coupling reaction that depends on tin organic reagents (stannanes) known as (Stille Coupling), maybe he would have shared the Nobel Prize if he didn't die at young age in 1989. [23] (Table 1.3).

Coupling reaction	Reaction name
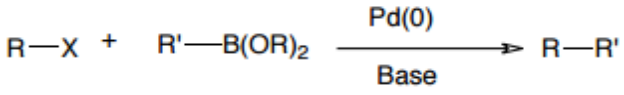	Suzuki[24]
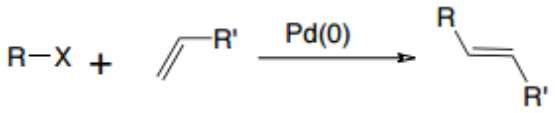	Heck [25]
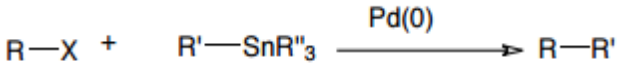	Stille [26]
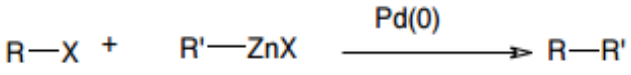	Negishi [27]
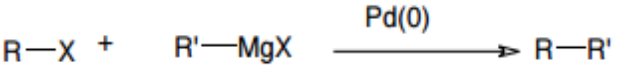	Kumada [21]

Table 1.3 Famous C-C Palladium based coupling reactions

These reactions give the highest results for aromatic halides and electron rich halide substrates rather simple alkyl structure. [28] They undergo similar palladium catalytic cycle except Heck Coupling that differs a little. [29] (Scheme 1.2).

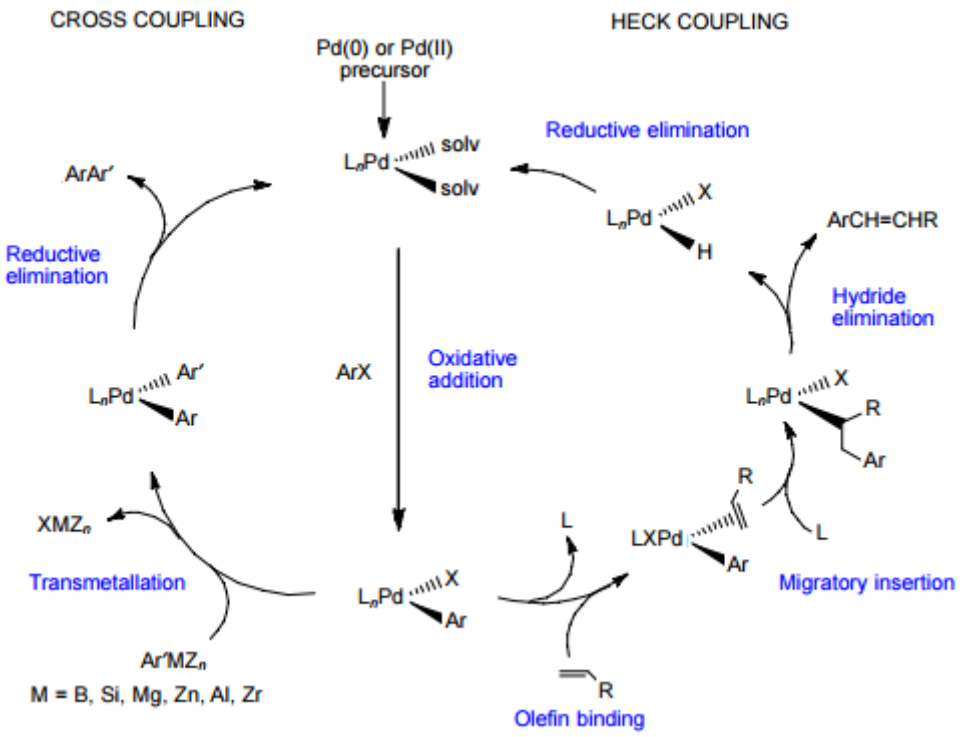

Scheme 1.2 Palladium Catalytic Cycle.

1.1.5 Applications

Conjugated materials are applicable in many fields that can roughly fall in two categories:

I- Electronic and optoelectronic:
e.g. Photovoltaic cells (solar cells), [30-31] Organic Light Emitting Diodes (OLED), [32] Thin Films Transistors (field-effect transistors (FETs)). [33]

II- Biological and biomedical applications
e.g. Drug delivering, [7]
Imaging cells and membranes for disease diagnosis, [34]
Cancer treating. [35]

1.2 Water soluble conjugated materials

Conjugated organic materials are highly hydrophobic structures, however, water soluble conjugated materials are organic materials with dual behavior that they have the conjugated backbone but they are water soluble at the same time. This combination comes from the chemical structure which consists of two parts; the hydrophobic conjugated backbone and the other part is water soluble moieties which are attached to the hydrophobic backbone as functional groups. [36,37] (Figure 1.5)

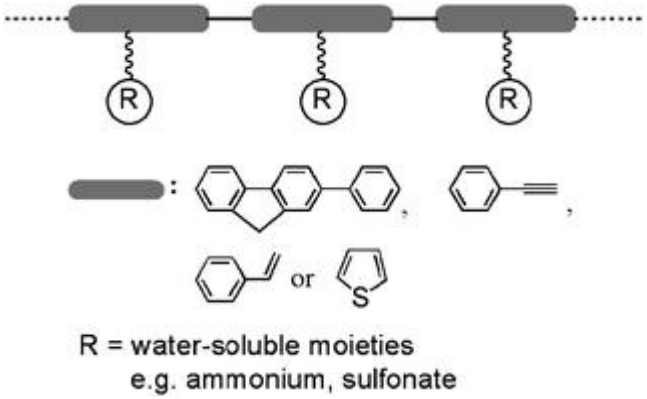

Figure 1.5 Water soluble conjugated polymers. Reproduced from Ref. 37 with permission from The Royal Society of Chemistry.

Forming water soluble conjugated materials got early attention from the beginning of establishing conjugated materials as branch of organic chemistry. Intensive researches were done by Heegar and other collaborators in 1980's on sulfonated polypyrroles and polythiophenes. [38] Water soluble functionalities varies from ionic moieties i.e. anionic: sulfonate, [39] phosphate, [40] acetate, [41] etc. cationic: ammonium. [42,43] Beside chemical groups there are hydrophilic molecules that are also used such as oligo/ polyethylene glycol, [44, 45] different monosaccharides, [46] cyclodextrines, [47] and cucurbiturils especially cucurbit[7]uril and cucurbit[8]uril .[48, 49] Choosing the kind of functionality may depend on the kind of target application of the final product. Introducing the water soluble functionality can be achieved by several ways; i- functionalizing the building block. Patrick van Rijn et al, [45] functionalized the monothiophene with tetraethylene glycol mono-methyl ether before bromination which was

followed by transformation to trimethylstannyl group and then was coupled through Stille Reaction (figure 1.6a). So as Bert de Boer *et* al [50] bifunctional bithiophene then polymerized obtaining regioregular polythiophenes with amphiphilic functionalities. (Figure 1.6b)

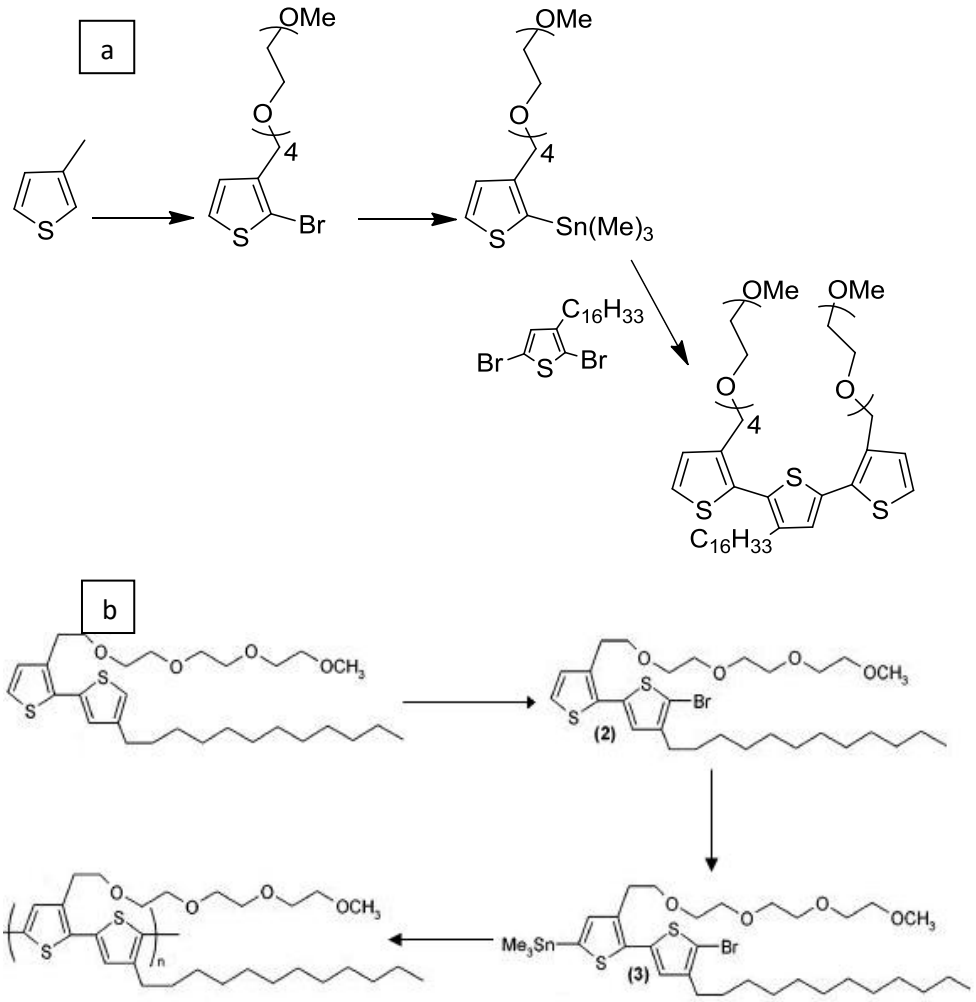

Figure 1.6a) Adapted from Ref [45]**, b)** Adapted from Ref [50]

ii- functionalizing the oligomer/ polymer instead. Deprotection of alcohol group of quaterthiophene in basic condition followed by etherification with mesylated methyltriethylene glycol in NaH. [51] (figure 1.7).

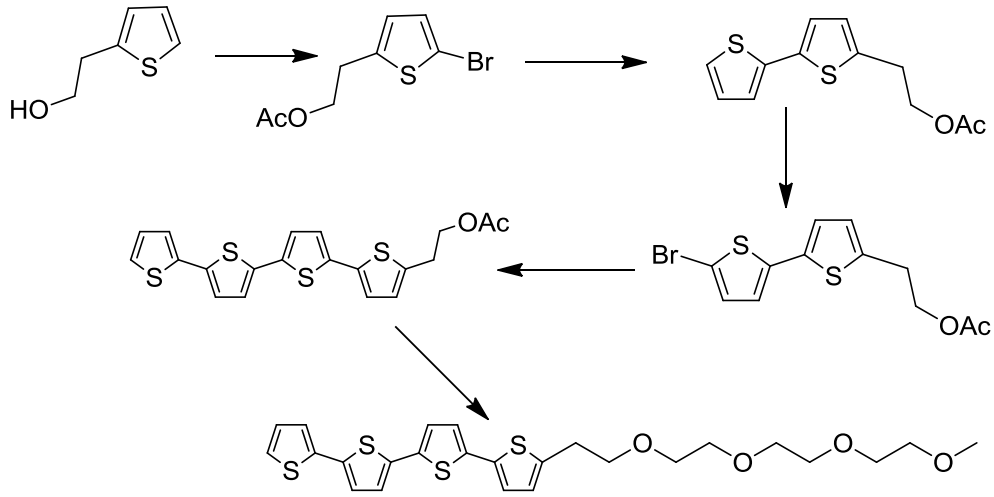

Figure 1.7 Quaterthiophene surfactant synthesis, Ref [51]

In a very common new method, click reaction (figure 1.8) is being widely used for the functionalization of conjugated macromolecules especially for functionalizing with monosaccharides, where most commonly the sugar would be propargylated and clicked with the azided side chain of the oligomer/ polymer. [52] The click reaction usually takes place by copper(I) catalization forming 1,4-triazole specie. (Figure 1.9)

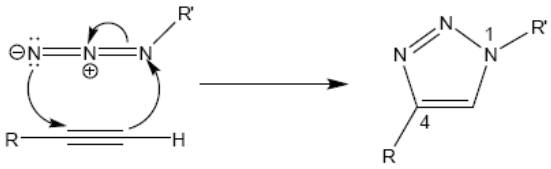

Figure 1.8 Click Reaction

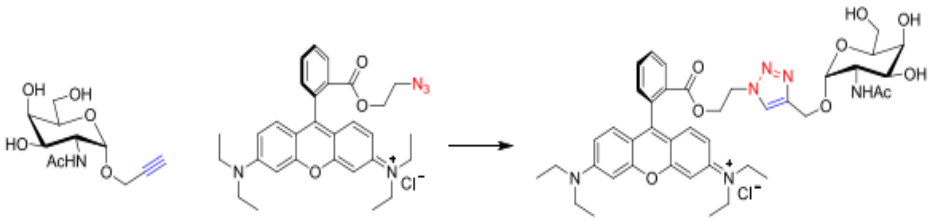

Figure 1.9 Clicking of azided dye chromophore to propargylated monosaccharide in DCM/acetone/H2O (v,v,v 6,4,1). Reproduced with permission from Ref [52] Copyright © 2013 WILEY-VCH Verlag GmbH & Co. KGaA, Weinheim.

Attaching the sugar to this structure in this case was done because of the application, where the compound is designed to target the interaction between this sugar related ligand with glycoprotein receptors on cancer cells. [52]

iii- The water soluble functionality may not be introduced by chemical bond, rather physical and electrostatic interaction by forming supramolecular compounds including rotaxanes and pseurotaxanes, these kinds of molecules are very common for cyclodextrines (β- dextrin) [47,53] and cucurbiturils [47,48,54] because of their hydrophobic gap that can encapsulate the hydrophobic chains by inclusion chemistry lows. [55]

Cyclodextrines are macro cyclic oligosaccharides class that have torus-like shape, referred to as CD. They are built up from α-D-glucopyranose units (figure 1.10) linked in (1- 4)-glycoside bonds. [56]

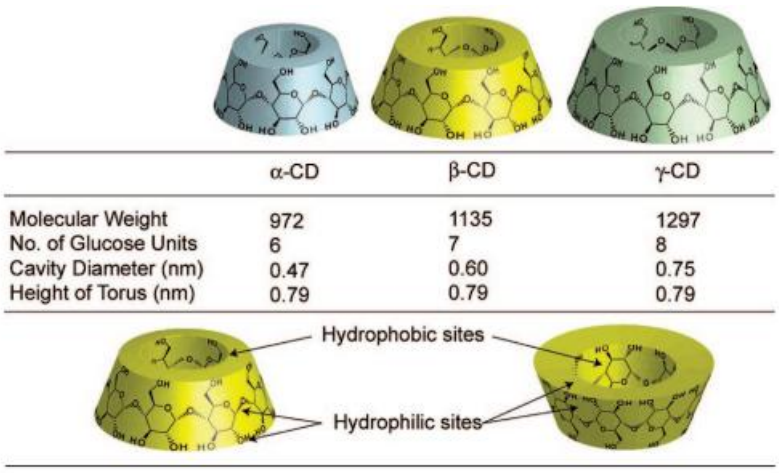

Figure 1.10 cyclodextrines, structures and physical properties. Reprinted (adapted) with permission from Ref [55]. Copyright (2009) American Chemical Society**.**

Hadziioannou et al [53], have synthesized oligothiophene- β- Cyclodextrin rotaxanes with stoppers forming water soluble rotaxanes. (Figure 1.11)

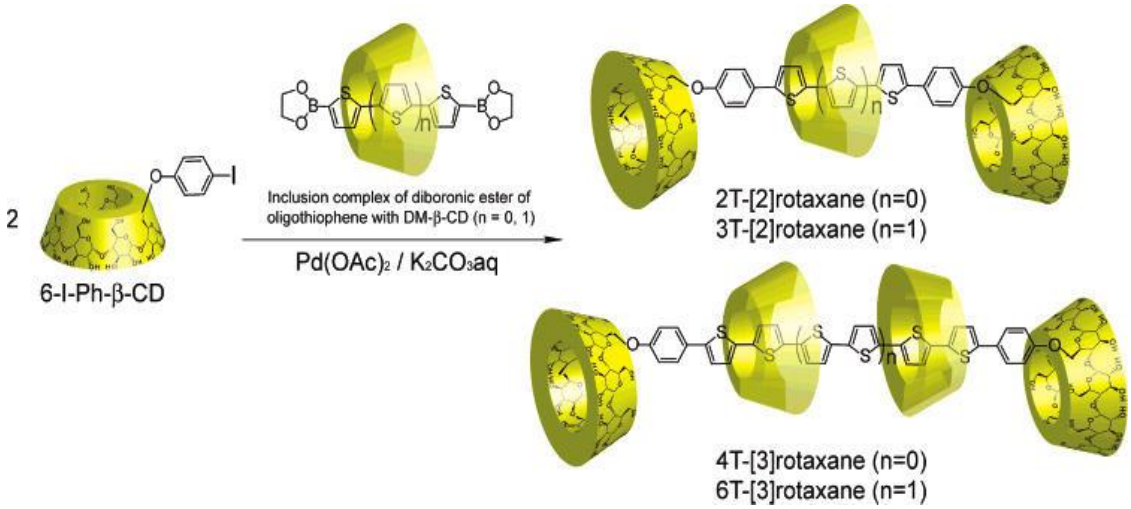

Figure 1.11 Rotaxanes formed by dimethyl-cyclodextrin and β-oligothiophenes (3,4,6,8) with β-Cyclodextrin Stoppers. Adapted with permission from Ref [53]. Copyright (2007) American Chemical Society.

Cucurbiturils, shortly referred to as CB[n] are built up from the condensation of glycoluril with formaldehyde (figure 1.12), [54-55] they share many similar properties with cyclodextrines. [56-57]

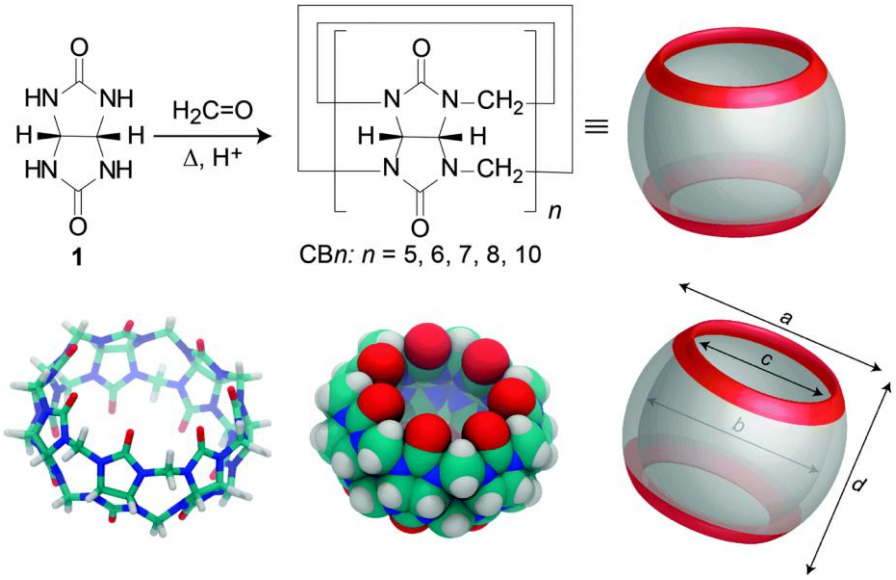

Figure 1.12 Cucurbit[n]uril structure and different kinds. Ref 54**,** Published by The Royal Society of Chemistry.

Tuncel et al, [48] synthesized conjugated structures and encapsulated parts of the backbone in CB8 which has big cavity, Carbonyl groups of CB8 are coordinated to protonated nitrogens of dimethyl groups in the polymer side chain (figure 1.13).

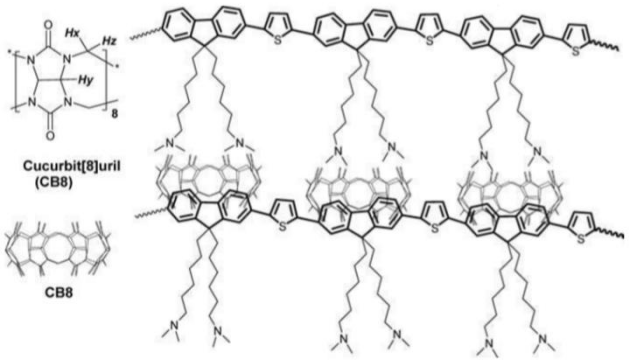

Figure 1.13 CB8 - polymer complex formation. Reproduced with permission from Ref [48] Copyright © 2010 WILEY-VCH Verlag GmbH & Co. KGaA, Weinheim.

1.3 Water dispersed conjugated materials nanoparticles

Conjugated materials nanoparticles (CMN) have show important witness for using conjugated materials in different fields. Their easy preparation, brightness, high quantum yield and low cytotoxisity. [58-59] Preparation of conjugated materials nanoparticles was reported by different groups, but in general falling under three catigories. [60-62]

Reprecipitation Method:

In reprecipitation method, conjugated material is dissolved in good solvent (THF, DMF) and rapidly added to excess amount of poor solvent (water). mixing the solvents causes sudden change in solvent quality which while doing disperssion with ultrasonicator, NP's of conjugated material particles can be formed. After the formation of nanoparticles, the solvent is removed which leaves NP's in the solvent (figure 1.14). The NP's formation driving force is hydrophobic effect. As discussed before, conjugated materials have long conjugated hydrophobic backbone, and with the absence of hyfrophilic groups, the hydrophobic chains

when put in highly polar medium i.e water, they tend to aggregate decreassing the interaction with water to the minimum level. [59-60] This aggregation is brough to its minimum when its thermodynamic conditions are most favorable, and this happens when conjugated backbone chains have collapsed conformations that form spherical particle shape. [63,64]

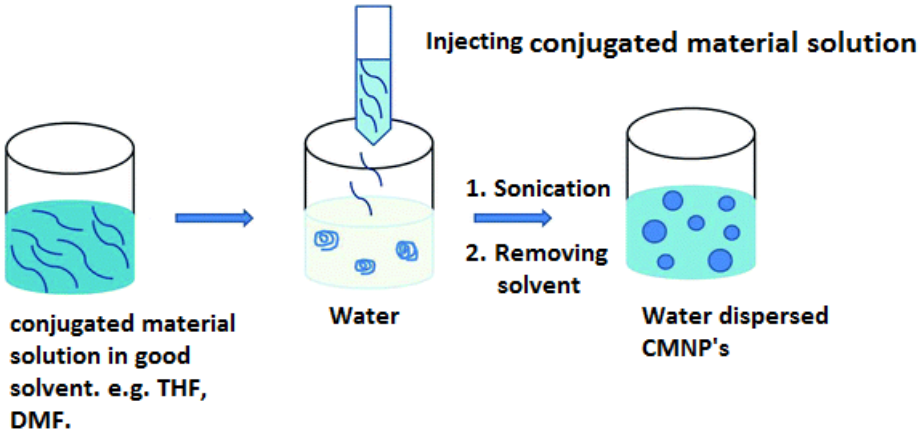

Figure 1.14 Reprecipitation method procedure, adapted from reference [65] with permission from The Royal Society of Chemistry.

This method can produce nanoparticles with sizes of 5-10 nm. [65]

Mini-emulsion Method:

This method differs from repricipitation method by using water immiscible solvent e.g. DCM, and more importantly applying a surfactant, the CM solution is injected into water with surfactant previously dissolved in it, with ultrasonication the two phases become miscible forming homogenous emulsions with conjugated material inside together (figure 1.15), when solvent is removed nanoparticles are formed stabilized by surfactant.

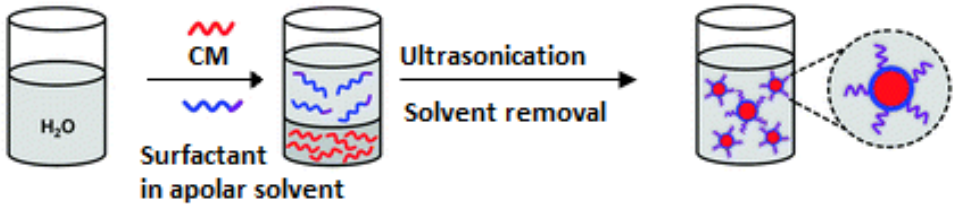

Figure 1.15 Mini-emulsion nanoparticles preparation procedure. Adapted from Ref. 58 with permission from The Royal Society of Chemistry.

The used surfactant varies for several reasons related to type of the conjugated material and the application, Peng Liu et al, [66] used PSMA (figure 1.16), obtaining nanoparticles with sizes 26 nm as measured by DLS technique. Other usages of surfactants were also reported such as polyethylene glycol PEG [67] and poly(DL-lactide-*co*-glycolide) PLGA. [68]

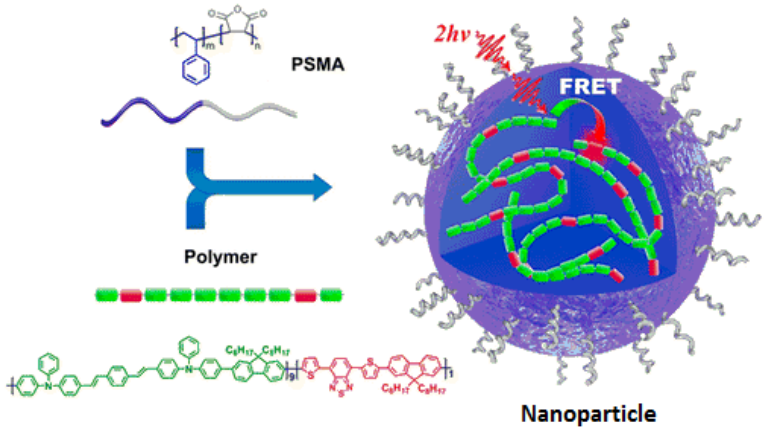

Figure 1.16 Nanoparticle formation by mini-emulsion method inside droplet of PSMA. Reprinted with permission from Ref 66. Copyright 2015 American Chemical Society.

Self-assembly is also a possible way for NP's preparation when conjugated materials have amphiphilic functionalities in the side chains that allow them to be self-assembled. [69]

All previous methods are considered postpolymerization; method which are applied after the chemical synthesis; less commonly but also widely common where polymerization is happened in heterophase systems. [62]

1.4 Biomedical applications of conjugated materials and thiophene based conjugated nanoparticles

In this section we spot the light on the importance of conjugated materials and their wide applications in biomedical field, [7, 34, 35, 37]. In order to apply any material to biological mediums, several conditions must be fulfilled; good biodegradability, biocompatibility, low cytotoxicity, and efficiency in aqueous mediums. Many researches on conjugated materials claimed their biodegredability especially for oligomers which can be consumed by macrophages, where chemical bonds are cleaved and later on to be cleared by the kidney. [70-73] this increases the importance of conjugated materials in biomedicine and bioimaging. Conjugated materials has been used for many biomedical regarding its emissive and conjugated backbone along with various functionalities related to the planned target that are bonded to the conjugated structure with chemical covalent bond [74] or non covalent bond [75] (Figured 1.17).

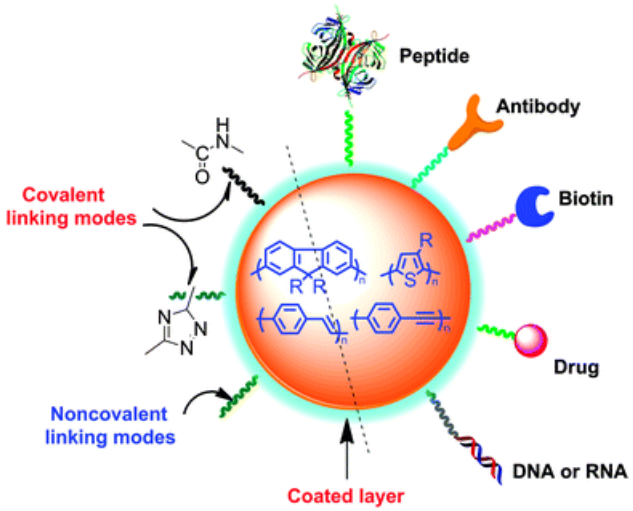

Figure 1.17 Biomedical Applications of Conjugated materials. Reproduced from Ref. 58 with permission from The Royal Society of Chemistry.

- **Cancer therapy and cancer drug carriers:**

The emissive backbone of conjugated materials has two major benefits in term of drugs and drug delivery: it was reported that light emitting conjugated materials have therapeutic activity when irradiated which open the doors for photodynamic therapy. [35, 76]

As drug carriers drugs can be loaded through covalent bond as in the research which was done by Shu Wang and collaborators [74] in 2011 who reported cisplatin covalently bonded to amphiphilic polythiophene structure and studied cisplatin distribution in cells (figure 1.18).

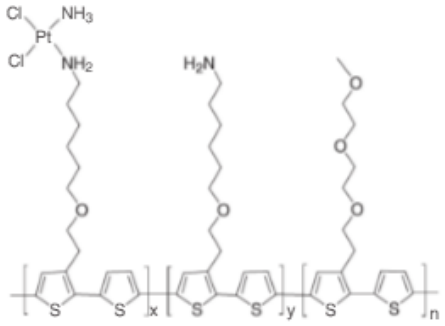

Figure 1.18 Amphiphilic polythiophene as cisplatin carrier. Ref [74]

Another study made by Shu Wang Group [77] reported in 2013; functionalized amphiphilic polythiophenes were used for intracellular targeting strategy. Polythiophene was designed and then the side chain was functionzlized through covalent bond with anticancer tyrosine kinase inhibitor lapatinib. To connect the polymer with the drug, oligomeric chain of poly(ethyleneglycole) is connected first to the side chain which will provide the water solubility to the molecule (figure 1.19)

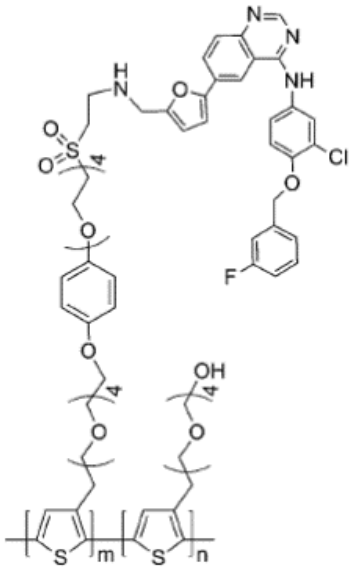

Figure 1.19 Amphiphilic polythiophene as lapatinib drug carrier. Reproduced from Ref. 77 with permission from The Royal Society of Chemistry.

The obtained molecule is used for cancer cells, since lapatinib can enter the intracellular domain of transmembrane epidermal growth factor receptor family proteins (figure 1.20).

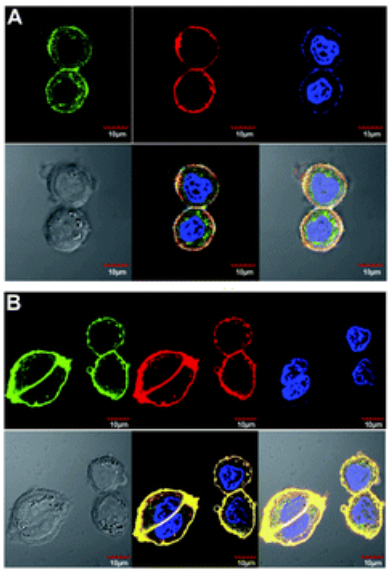

Figure 1.20 Cellular location of polyemer in different cell lines after 48 h of incubation: (A) SK-BR-3 cell line, (B) MCF-7 cell line. The false colors of polymer, Dil (cell membrane stain) and Hoechest 33258 (nucleus stain) are green,

red and blue respectively. The merged color of green and red is yellow. Reproduced from Ref. 77 with permission from The Royal Society of Chemistry.

It is observed that after loading the polymer by cells, this polythiophene is selectively targetting transmembrane proteins in the cell membrane, which in turn can be observed because of the selfluminous property of polythipophene.

Topoisomerase inhibitors are group of cancer drugs that inhibits the DNA topoisomerase in cancer cells preventing DNA replication which causes decomposition of DNA strands and apoptosis (programmed cell death) happens to cancer cells [78,79]. This group e.g Doxorubicin and Camptothecin of drugs are highly hydrophobic and toxic (figure 1.21), require carriers to be delivered.

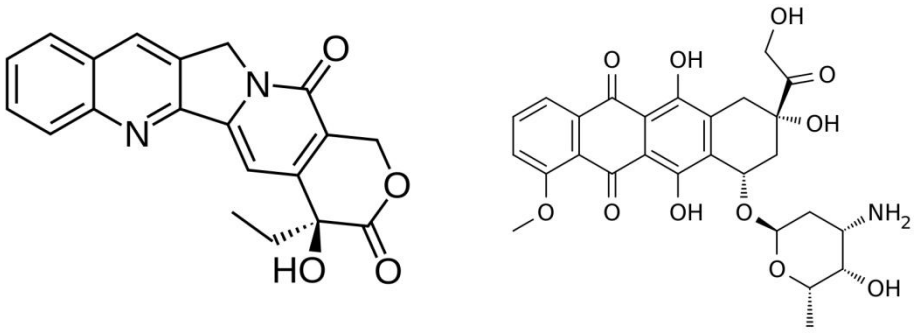

Figure 1.21 Camptothecin (left) and Doxorubicin (right)

Tuncel et al [49], reported in 2014 red emitting conjugated oligomer nanoparticles as camptothecin drug carrier. The cytotoxicity of was reduced by disguising amine groups in side chains with cucurbit[7]uril which caps the amine groups. Cucurbit[7]uril reduces the cytotoxicity and increases the stability of nanoparticles as water soluble functionality (figure 1.22). The drug is loaded on the backbone and bonded by π stacking of the two conjugated structures. The study showed that drug is being released more effectively at pH values lower than pH of blood (pH= 7.4).

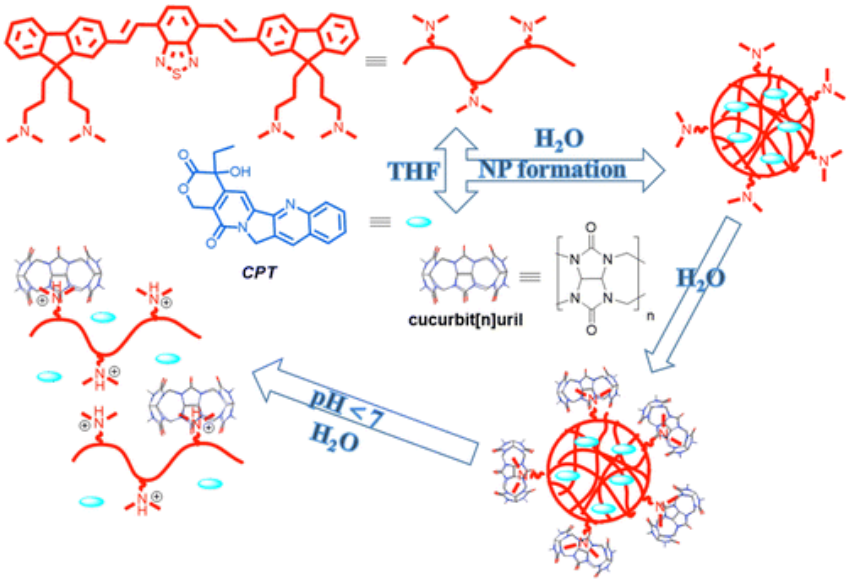

Figure 1.22 CB7 capped CPT drug-loaded nanoparticles and pH triggered drug release mechanism. Reprinted with permission from Ref [49]. Copyright 2014 American Chemical Society.

Releasing the drug in lower acidic pH medium gives selectivity to these nanoparticles considering the fact that cancer tissues are relatively acidic comparing to other tissues. [49]

- **Bioimaging and Diagnosis**

The imaging of nucleus and cytoplasm, cell membrane imaging is very important for studying cell morphology, structure and biological processes. Tracking theraputics in the cells and their interactions is also very important for divoloping the drugs and studying their effects on the tissues.

The market provides other options for *in vivo* imaging applications; quantum dots and organic fluorescence dyes, however, conjugated materials showed superiority comparing to the other materials. Quantum dots have the bright the most but they are risky because of their toxicity [80], organic dyes have been used for long years but their fluorescence property is weak and their compatibility in the biological systems is relatively low. On the other hand, as previously explained, conjugated materials have showed low cytotoxicity and stability in biological mediums. Anderson and coworkers in 2015 [81], developed thiophene based dyes for

imaging living cells and they compared their study with commercially available dye organic FM4-64. (figure 1.23)

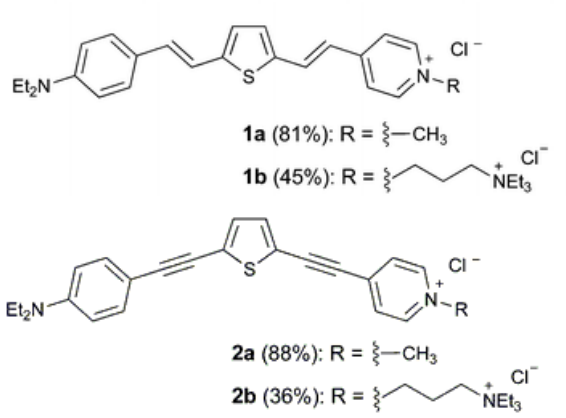

Figure 1.23 Thiophene-based dyes for cell imaging adapted from ref [81]

Thiophene cycle acts as a conjugated bridge, The 4-(diethylamino)phenyl substituent is used as an electrondonor, while a pyridinium group acts as the electron-acceptor, the positive head of ammonium helps to prevent the dye from penetrating the cell membrane and defuse incide. Moreover, the polar head increases the polarity of the dye which is more preferable for the cell. Hence, the dyes localize in lipid bilayer membranes, and that they become more fluorescent when they insert into the membrane. The toxicity studies showed that the doubly-charged dyes are not showing notable light or dark toxicity, whereas the singly-charged dyes are phototoxic even at very low concnetrations (figure 1.24), and this is probably due to the high rates of intracellular uptake, and singlet oxygen production of these structures.

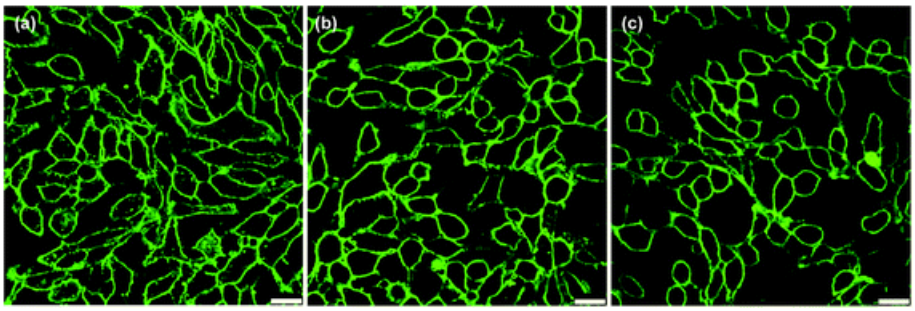

Figure 1.24 Confocal laser scanning microscopy images of living cells with green dyes. right: commercial organic dye/ middle: 1b and left: 2b. Reproduced from Ref. 49 with permission from The Royal Society of Chemistry.

Using thiophenes for imaging goes beyond only imaging the cells, it can be used to image any desired subject in the system by the optical properties of the conjugated backbone and the functionality that is functioned with. One of these is imaging distorted aggregated proteins which is considered as diagnosis of some related diseases that is caused upon the aggregated protein. [82] In 2009 Aslund *et* al reported synthesis of pentameric thiophene derivatives, denoted luminescent conjugated oligothiophenes (LCOs), which could be used for real time imaging of cerebral protein aggregates in transgenic mouse models of neurodegenerative diseases by multiphoton microscopy, LCOs showed selective strike for protein aggregates associated with prion diseases. [41] Some of the synthesized oligomers efficiently crossed the brain blood barriers (BBB). The motive for this study was to find a noninvasive way to detect the aggregated amyloid that can be detected by engineering chemical structures that can cross the BBB which require small less polar units comparing to the polymers which were prepared and studied in previous publications (poly thiophenes with polar side chains). [83] The study applied the oligomers *in vivo ex vivo* and *in vitro* for both mice brain and humans'. (figure 1.25) and (figure 1.26) show the chemical structures and results for *ex vivo* studies on mice brain sections.

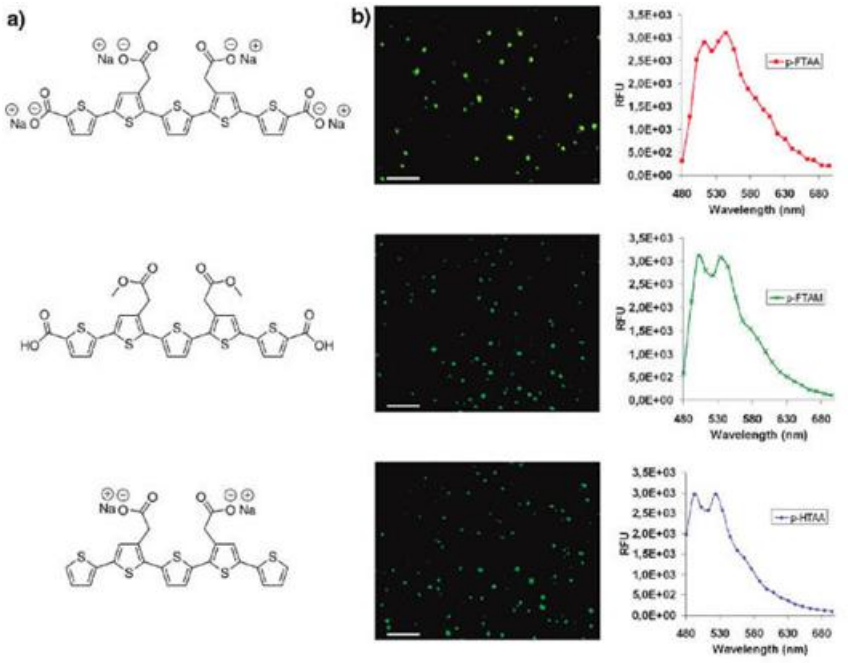

Figure 1.25 Pentathiophene chemical structures, their emission spectras, and fluorescence images after binding to Aβ deposits in formalin-fixed tissue samples from transgenic mice with AD pathology and *ex vivo* imaging of protein deposits in mice after intravenous or intracerebral injections Fluorescence images and emission spectra of Aβ deposits in tissue sections of mice brains. Adapted with permission from Ref [41]. Copyright 2009 American Chemical Society.

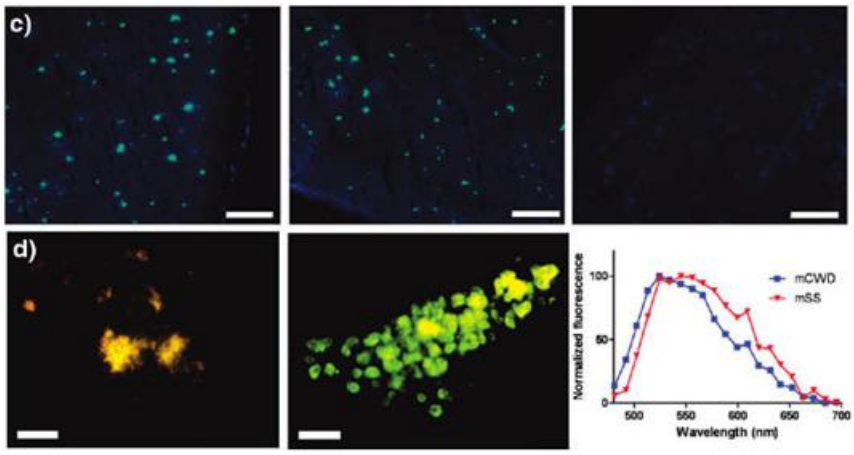

Figure 1.26 *Ex vivo* fluorescence images of cerebral amyloid plaques in brain sections. Adapted with permission from Ref [41]. Copyright 2009 American Chemical Society.

The least hydrophilic compound (the middle structure) showed the lowest crossing ability to brain blood barriers comparing to the anionic other two pentamers, which make it possible to conclude that the esterfication of the carboxyl groups is necessary for active transport of these oligomers over the brain blood barriers.

1.5 Aim of the thesis

In this study, the aim is to synthesize macromolecule that combine several properties; an emissive hydrophobic backbone, water solubility and availability for biological systems i.e. biodegradability, low cytotoxicity, and biocompatibility. This combination was performed by synthesizing oligomer of conjugated four units of thiophene which fulfill the emissive requirement then it was functionalized with polyethylene glycol [1500] which act as amphiphilic functionality that makes the molecule water soluble as a whole.

In order to apply it to biological mediums nanoparticles in water were synthesized starting from the well defined chemical formula.

Chapter 2

EXPERIMENTAL

2.1 Materials

All solvents and reagents were used without any treatment unless mentioned, all column chromatography purifications were conducted using silica gel (Kieselgel 60, 0.063 – 0.200 nm) Merck, and were monitored by thin layer chromatography silica gel plates (Kieselgel 60 F254, 1mm) Merck, under short wave length or long wave length UV lamp (254 nm and 365 nm) respectively. Sephadex (G-15 medium) was used to purify P1.

2.2 Instrumentation

2.2.1 Mass Spectroscopy

Mass of synthesized materials were determined using Agilent 6224 Mass Spectroscopy Time of Flight TOF LC/MS with electrospray ionization.

2.2.2 ^{1}H-NMR, ^{13}C-NMR and 2DNMR

All NMR characterizations for references, monomers, oligomers and polymer were done using various deuterated solvents with Bruker Avance DPX-400 MHz Spectrometer. The chemical shifts of the spectrums were expressed relative to tetramethylsilane as internal standards.

2.2.3 FT-IR Spectroscopy

The IR spectrum was recorded to characterize the chemical shifts of the oligomers, Fourier Transform Infrared Spectra was measured using Bruker-ALPHA Spectrometer. The samples were scanned 64 times and collected at room temperature by adjusting the range as 4000 cm^{-1}- 400 cm^{-1} with scanning resolution previously set at 4 cm^{-1}.

2.2.4 UV-VIS Spectroscopy

Cary 300 UV-VIS Double Beam Spectrometer equipped with Xenon- lamp as light source was used to measure the UV absorbance of oligomers and polymer dissolved in various solvents using 1 cm in width quartz cell cuvettes.

2.2.5 Photoluminescence Spectroscopy

The PL Spectrums the different solutions of oligomers and polymer were recorded in 1 cm width quartz cell cuvettes, using Cary Eclipse Varian Spectrophotometer and Xenon lamp as light source. All measurements were recorded with excitation wavelength of the UV related λ_{max}.

2.2.6 Dynamic Light Scattering (DLS)

DLS method was used to determine the size of the nanoparticles. All solutions where prepared in double distilled water at 25^{o} C in disposable DLS 1 cm width, using Zetasizer Nano-ZS instrument.

2.2.7 Environmental Scanning Electron Microscopy and Transmission Electron Microscopy

The morphology and shape of nanoparticles were studied by using Environmental Scanning Electron Microscopy (ESEM) Quanta 200 FEG and Transmission Electron Microscopy instrument (TEM), FEI Tecnai G2 F30.

2.3 Synthesis

2.3.1 Synthesis of M1, 2-(5-bromo-2-thienyl)ethanol from 2-(2-thienyl) ethanol:

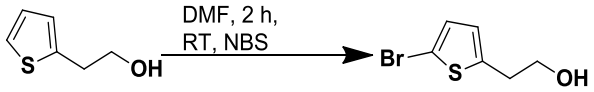

To a 6 ml of degassed DMF, NBS (N-bromosuccinimide) (1.66 g, 9.3 mmol) was added and dissolved well to obtain pale yellow solution. Separately, to a 50 ml round bottom flask, 2TE (2-(2-thienyl) ethanol) (1 g, 7.8 mmol) was dissolved in 6 ml degassed DMF. NBS solution was added drop wise within 2-3 minutes to the 2TE solution on a stirrer. The reaction was left for 2 h in an inert atmosphere at room temperature in dark by wrapping the flask with aluminum foil.

The progress of the reaction was monitored by thin layer chromatography, (TLC). After the reaction was completed, it was quenched with ice and then dd water/ DCM extraction was done. The DCM solution was passed through silica layer performing silica filtration, followed by evaporation of solvent under reduced pressure producing viscous pale yellow product which was finally dried under vacuum giving yield 1.3186g (81%).

R_f values: (2TEBr 0.5125, 2TE: 0.5625; eluent 3:7 EtOAc: cyclohexane).

UV λ_{max} = 228nm in DCM.

^{1}H-NMR (400 MHz, $CDCl_3$, 25 ^{o}C) δ ppm, 6.91 (Ar, d, J= 3.6 Hz, 1H), 6.65 (Ar, d, *J*= 3.6 Hz, 1H), 3.84 (CH2CH2OH, t, *J*= 6.2 Hz, 2H), 3.0 (ArCH2CH2, t, *J*= 6.2 Hz, 2H).

^{13}C-NMR (100 MHz, $CDCl_3$, 25 ^{o}C) δ ppm: 142.8, 129.7, 126, 109.9, 63, 33.7.

2.3.2 Synthesis TET1 of 2,2'-([2,2':5',2'':5'',2'''-quaterthiophene]-5,5'''-diyl)diethanol through Stille coupling:

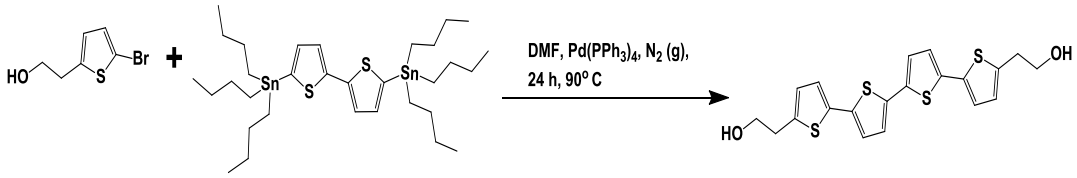

To 25 ml 2-neck round bottom flask, 2-(5-bromothiophen-2-yl)ethanol M1 (0.60 g, 2.89 mmol) and 5,5'-bis(tributylstannyl)-2,2'-bithiophene (0.98 g, 1.32 mmol) were added. The mixture was dissolved in 4 ml of dry DMF, and the contents of the flask were subjected to three cycles of freeze pump thaw technique, for degassing and filled with N_2. Then Pd(PPh3)4 catalyst (0.076 g, 0.066 mmol) was added and the reaction was heated to 90 ^{o}C for 24 h N_2 in dark.

The reaction crude was washed with THF and Silica-filtration was applied to the crude, then all solvents were evaporated under reduced pressure, to the viscous resulted liquid, cyclohexane was added and the mixture was washed several times on a centered-glass. After collecting the material, precipitation technique was applied in cold ethanol after dissolving TET1 in smallest amount of THF then dropped on excess amount of cold ethanol and left in the ethanol overnight in fridge for better separation, then the ethanol was removed by decantation resulting in dark yellowish fine solid. The precipitation was repeated for maximum recovery of material from ethanol, finally the product was collected and dried under vacuum giving 447 mg (75% yield).

R_f value (0.375 ;eluent 1:1 cyclohexane: EtOAc).

^{1}H-NMR (400 MHz, $CDCl_3$, 25 ^{o}C) δ ppm: 7.02 (Ar, m, 3H), 6.80 (Ar, d, *J*= 3.6 Hz,1H) 3.90 (CH2CH2OH, t, *J*=6 Hz, 2H), 3.08 (ArCH2CH2, t, *J*=6.4 Hz, 2H).

^{13}C-NMR (100 MHz, DMSO(D6), 25 ^{o}C) δ ppm: 142.3, 135.7, 134.5, 126.8, 124.5, 124.0, 62.1, 33.7.

LC/MS HRMS-TOF: (MeCN, positive mode detection) M calculated= 418.018 m\z , found= 418.016 m\z, error= 6.9 ppm, (M+1) 419.018 25.5%, (M+2) 420.013 21%, (M+3) 421.114 13%

UV- VIS: Absorbance λ_{max}= 367 nm in $CHCl_3$ [blue-green emitting].

PL, λ_{max}= 445 nm excitation @ λ_{max}= 367 nm.

2.3.3 Synthesis of P1, 2,2'-([2,2':5',2'':5'',2'''-quaterthiophene]-5,5'''-diyl)poly(ethyleneoxide)

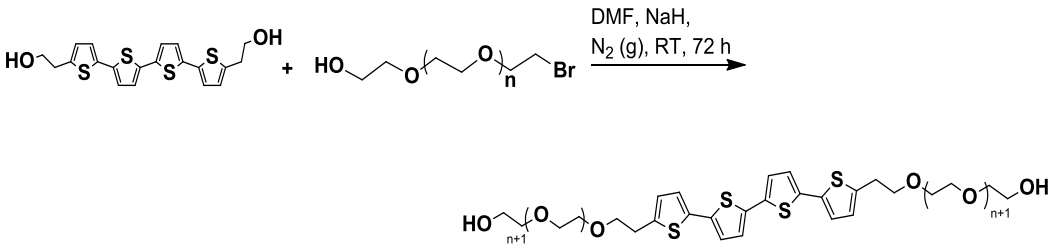

In a 25 ml two neck-round bottom flask, TET1 (27.0 mg, 0.0645 mmol) was dissolved in dry degassed DMF (3 ml), then NaH (8.0 mg, 0.3225 mmol) was added under N_2 flow and stirred for 1 hour, after that bromine terminated polyethylene glycol (248.2 mg, 0.1655 mmol) was separately dissolved in (3 ml) of dried degassed DMF, to obtain a clear solution, and then the resulting solution was injected into the reaction flask and the reaction mixture was stirred at room temperature in dark for 3 days.

After 3 days excess NaH was quenched with MeOH and stirred for 5 minutes, then all solvents were evaporated under reduced pressure. Finally, the solid residue was purified through Sephadex column using dd water as eluent. After collecting the material, water was evaporated under reduced pressure and dried under vacuum to afford orange powder (70 mg).

^{1}H-NMR (400 MHz, $CDCl_3$, 25 ^oC) δ ppm: 7.5- 7.75 Aromatic ,3.5- 3.8 CH2CH2O.

UV- VIS: Absorbance λ_{max}= 367 nm (in chloroform), λ_{max} = 372 nm (in water).

PL excitation @ $\lambda_{max=}$ 367 nm (in chloroform), λ_{max} = 372 nm (in water) respectively gave emissions: λ= 445 nm and λ= 455 nm

2.3.4 Synthesis of M2, 2-(2-bromothiophen-3-yl)ethanol:

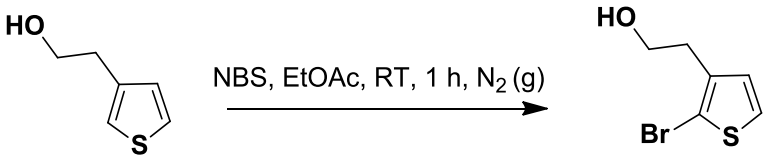

In 100 ml 2-neck round bottom flask NBS (3.20 g, 0.018 mmol) was dispersed for 10 minutes in 30 ml of degassed ethylacetate using sonicator. 2-(thiophen-3-yl)ethanol (2.0 g, 0.0156 mmol) was injected into the flask and the reaction was left for 1 h in the sonicator in an inert atmosphere at room temperature in dark. After that EtoAc/H_2O extraction was done, then solvent was evaporated under low pressure. the obtained crude was purified by column chromatography with the material coming collected second. After evaporating the solvents, the sample was dried under vacuum which afforded pale yellow viscous liquid 0.88 g (27%).

R_f value: (0.45 ; eluent 3:7 EtOAc: cyclohexane).

^{1}H-NMR: (400 MHz, $CDCl_3$, 25 ^{o}C) δ ppm, 7.26 (Ar, d, *J*= 5.6 Hz, 1H), 6.89 (Ar, d, *J*= 5.6 Hz, 1H), 3.87 (CH2CH2OH, t, *J*= 7.2 Hz, 2H), 2.90 (ArCH2CH2, t, *J*= 6.4 Hz, 2H).

2.3.5 Synthesis of M3, 2-(5-bromo-2-thienyl)ethyl 4-methylbenzenesulfonate:

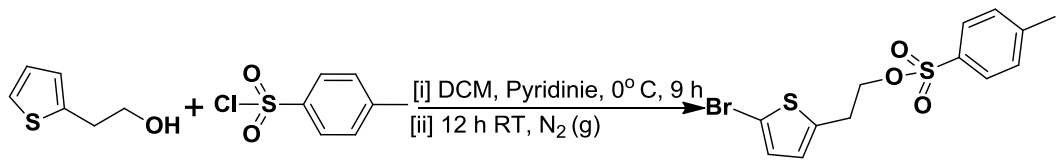

Previously synthesized M1 2-(5-Bromo-2-thienyl)ethanol (1.02 g, 4.9 mmol) was dissolved in 20 ml of dry DCM, in a 100 ml round bottom flask. The mixture was stirred under N_2 at 0^O C, and then tosyl chloride (1.409 g, 7.4 mmol), pyridine (0.8

ml, 9.85 mmol) were added respectively. Reaction mixture was left under nitrogen at 0 ^{o}C for 9 h, then left at room temperature overnight.

Workup: dd Water/DCM extraction, then consecutively the reaction mixture was washed with water, hydrochloric acid 1 M, sodium bicarbonate 1 M, after that it was dried over anhydrous sodium sulfate. The obtained mixture was purified using column chromatography, the final obtained product was white solid crystals. The reaction gave yield 57%, and (0.25 g, 25% non-reacted starting material was recovered from the column).

R_f= 0.6 (EtOAc :Cyclohexane 3:7)

^{1}H-NMR (400 MHz, $CDCl_3$, 25 ^{o}C) δ ppm: 7.74 (Ar-tosyl, d, *J*= 8.4 Hz, 2H), 7.34 (Ar-tosyl, d, *J*= 8 Hz, 2H), 6.85 (Ar, d, J= 3.6 Hz, 1H), 6.58 (Ar, d, J=4 Hz, 1H), 4.20 (CH2CH2OH, t, *J*= 6.4 Hz, 2H), 3.1 (ArCH2CH2, t, *J*= 6.6, 2H), 2.48 (CH3, s, 3H).

^{13}C-NMR (100 MHz, $CDCl_3$, 25 ^{o}C) δ ppm: 144.9, 140.0, 132.8, 129.8, 129.7, 127.9, 126.6, 110.6, 69.6, 29.94, 21.7.

2.3.6 Synthesis of TET2, [2,2':5',2'':5'',2'''-quaterthiophene]-5,5'''-diylbis(ethane-2,1-diyl) bis(4-methylbenzenesulfonate]:

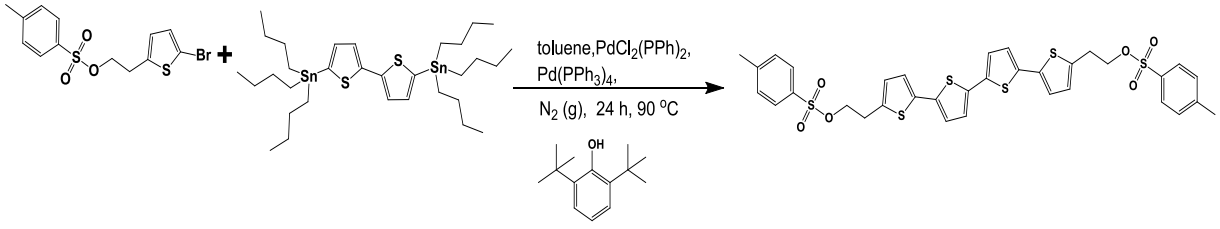

To a 50 ml two neck round bottom flask, M3 (0.500 g, 1.38 mmol) and 2,6-ditertbutylphenol (2.1 mg, 0.0101 mmol) were added and dried under vacuum for 30 min. 15 ml of degassed toluene was added along with 5,5'-bis(tributylstannyl)-2,2'-bithiophene (0.4891 g, 0.657 mmol) to the reaction mixture and stirred till obtaining homogeneous mixture. The reaction mixture was subjected to 3 times freeze- thaw technique as described before (2.3.2). After that the catalysts were added $PdCl_2(PPh_3)_2$ (0.023 g, 0.033 mmol) and $Pd(PPh_3)_4$ (0.022 g, 0.019 mmol)

under flow of N_2, then the reaction was kept under light flow of N_2 at 90^oC for 24 h in dark.

The red colored reaction mixture was cooled down to room temperature and then, under reduced pressure solvent was removed. The residue was washed with water followed by $CHCl_3$/ H_2O extraction, after that chloroform was removed under reduced pressure. The remaining solid was dissolved in smallest amount of THF and the solution was dropped on excess amount of cold methanol and left overnight in fridge for better separation. Then using decantation technique, the solvent precipitates were collected and dried under vacuum, orange colored fine powder was obtained. 0.2235 g (48%).

^{1}H-NMR (400 MHz, $CDCl_3$, 25 ^oC) δ ppm: 7.76 (Ar-tosyl, d, *J*= 8.4 Hz, 2H) 7.32 (Ar-tosyl, d, *J*= 8.8 Hz, 2H) 7.07 (Ar, d, *J*=4 Hz, 1H) 7.00 (Ar, d, *J*=4 Hz, 1H) 6.97 (Ar, d, *J*=3.6 Hz, 1H) 6.73 (Ar, d, *J*= 3.6 Hz, 1H) 4.26 (CH2CH2OSO2, t, *J*=6.6 Hz, 2H) 3.16 (ArCH2CH2, t, *J*=6.4 Hz, 2H) 2.42 (s, 3H).

^{13}C-NMR (100 MHz, $CDCl_3$, 25 ^oC) δ ppm: 21.6, 29.9, 69.9, 123.5, 124.1, 124.2, 127.1, 127.9, 129.8, 132.9, 135.7, 136.1, 136.2, 137.8, 144.9.

LC/ MS- HRMS time of flight: MeOH as solvent, Vcap 3500 V, [M+H$^+$] calcd for $C_{34}H_{30}O_6S_6$ 727.04 m\z, found: 727.042 m\z, error: 2.41ppm. (M+1) 727.04 (100%), (M+2) 728.04 (41.34%), (M+3) 729.04 (34.13%), (M+4) 730.04 (11.75%).

UV-VIS: Absorbance λ_{max}= 400 nm (in chloroform), PL λ_{em}= 490 nm (in chloroform) excitation @ λ_{max}= 400 nm

2.3.7 Synthesis of TET3, 5,5'''-bis(2-azidoethyl)-2,2':5',2'':5'',2'''-quaterthiophene:

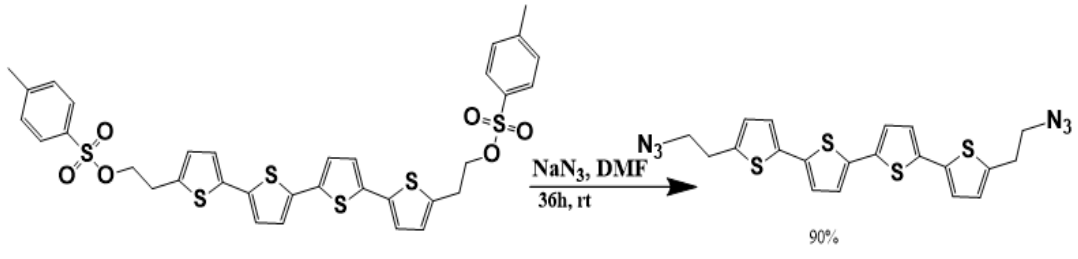

To a 10 ml round bottom flask, TET2 (50 mg, 0.068 mmol) was added and dissolved in 3 ml of warm DMF (to increase the solubility). Then sodium azide (26.83 mg, 0.412 mmol) was added and stirred at room temperature for 36 hours.

After reaction was over, DMF was evaporated under reduced pressure, the resulting orange solid was washed with water several times, filtered, then dried under vacuum to afford orange colored solid (40mg, 90%).

R_f= 0.675 eluent: 3:7 EtOAc: Cyclohexane.

UV- VIS: Absorbance λ_{max} = 405 nm in $CHCl_3$

^{1}H-NMR (400 MHz, $CDCl_3$, 25 ^oC) δ ppm: 7.0 to 7.15 (Ar, m), 6.82 (Ar, d, *J*= 3.48 Hz, 1H) 3.12 ($ArCH_2CH_2$, t, *J*= 6.88 Hz ,2H) 3.59 (CH_2N_3, t, *J*= 6.84 Hz, 2H)

2.3.8 Nanoparticles preparation and characterization:

2.3.8.1 P1 nanoparticles preparation and characterization using reprecipitation method (sonication)

300 µl solution of P1 (0.2 mg.ml^{-1}) in THF was injected into 10 ml of dd water while sonicating and kept subjected to sonication for a total of 1 hour, forming 0.02 mg.ml^{-1} concentration. THF was evaporated under reduced pressure at room temperature. The characterizations were done by DLS dynamic light scattering, TEM and SEM.

2.3.8.2 P1 nanoparticles characterization and preparation using repricipitation method (stirring):

300 µl solution of P1 (0.2 mg.ml^{-1}) in THF was injected into 10 ml of dd water while stirring using magnetic stirrer and kept stirred for a total of 1 hour, forming 0.02 mg.ml^{-1} concentration. THF was evaporated under reduced pressure at room temperature. The characterizations were done by DLS (Zeta Sizer), TEM and SEM.

2.3.8.3 P1 nanoparticles preparation by self-assembly

A fresh solution of P1 (0.2 $mg.ml^{-1}$) in water was freshly prepared and used as stock solution. various concentrations (0.025, 0.01, 0.02, 0.04, 0.06) were prepared by injecting the stock solution in water to a total volume of 10 ml while stirring for an hour.

2.3.9 Quantum Yield calculation (η)

Quantum Yield: 19.81% +\- 1.67 using THF as solvent; was calculated at an excitation wavelength of 367 nm using a Spectral Products monochromator integrated xenon lamp, an Ocean Optics Maya 2000 spectrometer and a Hamamatsu integrating sphere, where used as the following: 1- the measurement of the spectrum when there is no sample placed in the integrating sphere, 2- The measurement of the spectrum when the sample is directly illuminated by the excitation source, 3- The measurement of the sample when the sample is illuminated by the light scattered from the surface of the integrating sphere (indirect illumination). [84]

$$\eta = \frac{L_2 - \frac{E_2 L_3}{E_3}}{\left(1 - \frac{E_2}{E_3}\right) E_1}$$

E: Excitation part of the spectrum.

L: Emission part of the measured spectrum.

Chapter 3

RESULTS AND DISSCUSSIONS

Introduction:

The discussion part will be divided into two parts. The first part will discuss the chemical synthesis and characterizations of the monomers, oligomers and the macromolecule. In the second section preparation and characterization of nanoparticles will be studied.

3.1 Section1: Synthesis of P1 Thiophene- Based Tetramer Functionalized With Polyethylene Glycol (PEG-TET-PEG)

The aim of the study is to synthesize conjugated structure (thiophene based) with water soluble ability which was performed by introducing bromine terminated polyethylene glycol (Avg Mw: 1500 g/mol) to the tetramer from both sides forming macromolecule with experimentally proved long- period stable good water solubility (0.1 mg/ml). These water soluble structures have the ability to form self- assembled nanoparticles without the need to use extra solvent as usually used in conjugated materials nanoparticles preparation methods (miniemulsion and reprecipitation).

The synthesis was conducted by introducing bromine to the only available α position of 2-(2-thienyl) ethanol, in order to couple the thiophene ring with bithiophene and form tetramer. After the tetramer structure was formed, the hydroxyl groups were activated by abstracting the protons with strong base and by S_N2 mechanism nucleophilic substitution with bromine terminated polyethylene glycol from one side, P1 was formed. (Scheme 3.1) shows the outline of the synthesis.

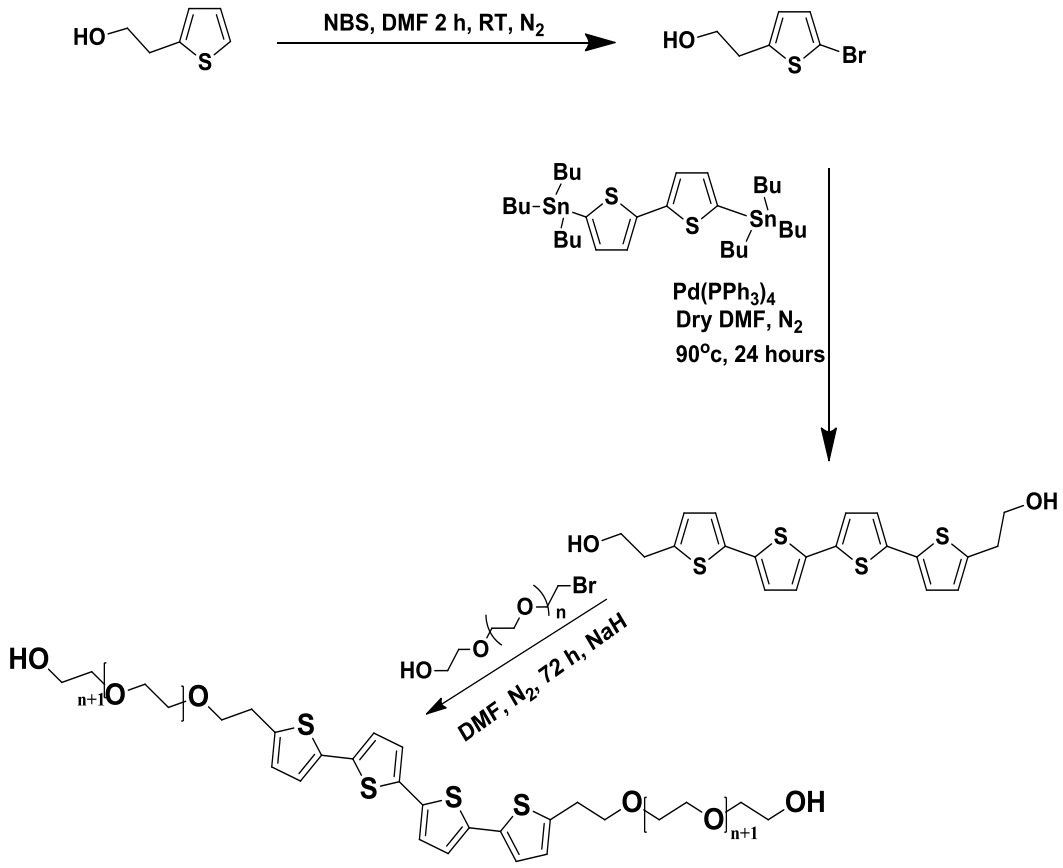

Scheme 3.1 The outline of P1 synthesis

3.1.1 Synthesis of M1, 2-(5-bromo-2-thienyl)ethanol from 2-(2-thienyl) ethanol:

Figure 3.1 M1 physical appearance.

As was mentioned in the introduction; among the five- membered aromatic heterocyclic compounds, thiophene has the most aromatic behavior, therefore it is the least active comparing to pyrrole and furan. However, using N-bromosuccinimde with the reactive N-Br polar bond, exothermic bromination reaction can be performed easily through electrophilic substitution to the only available one α position, which is more favorable, giving one possible product as described in the mechanism shown below in (scheme 3.2)

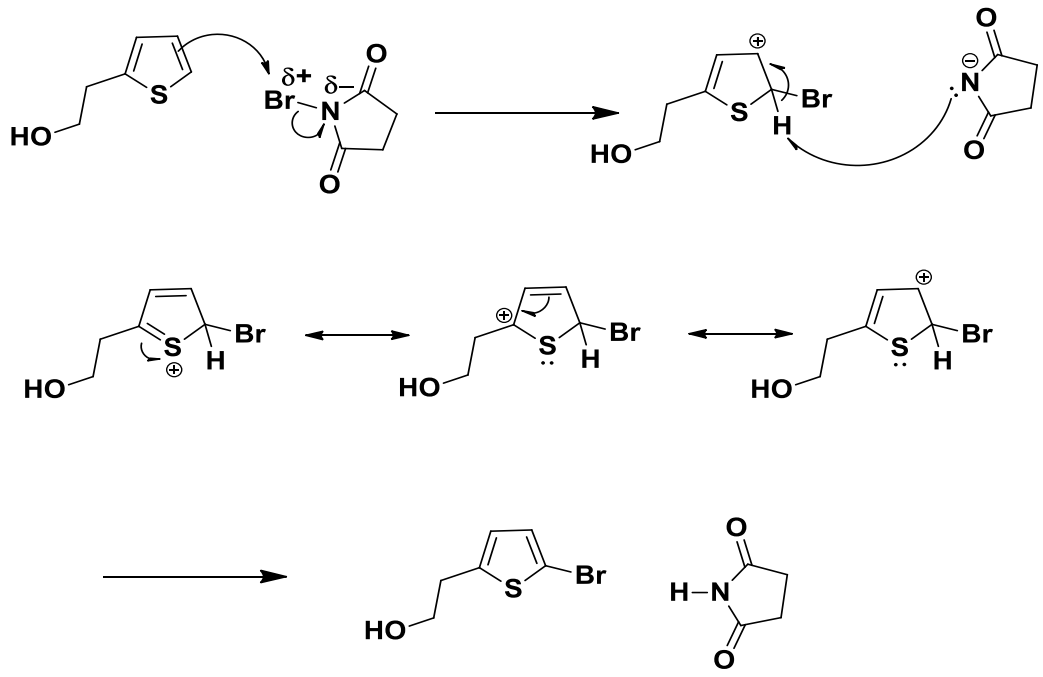

Scheme 3.2 Bromination reaction of from 2-(2-thienyl) ethanol

The structure of the product was characterized by both ^{1}H-NMR and ^{13}C-NMR (figure 3.3) and (figure 3.4) respectively. In the ^{1}H-NMR spectrum of the starting material 2-(2-thienyl) ethanol (figure 3.2), the three aromatic protons (doublet, triplet, doublet) are shown between (6.8- 7.2 ppm), while the two triplets at 3.0 ppm and 3.84 ppm represent the aliphatic protons, with the consideration that the aliphatic methylene neighboring the hydroxyl group is more deshielded (3.9 ppm).

After introducing the bromine group to the structure, the proton attached to the carbon at position 5 was substituted with the bromine and was completely disappeared from the spectrum, therefore the triplet at 7.0 ppm became doublet.

Moreover, changing the environment of the protons by the bromine addition, decreases the aromatic protons shifting to lower ppm values, without having much affection on the separation between the aliphatic methylenes, having the fact that bromine position relatively far from the ethyl group.

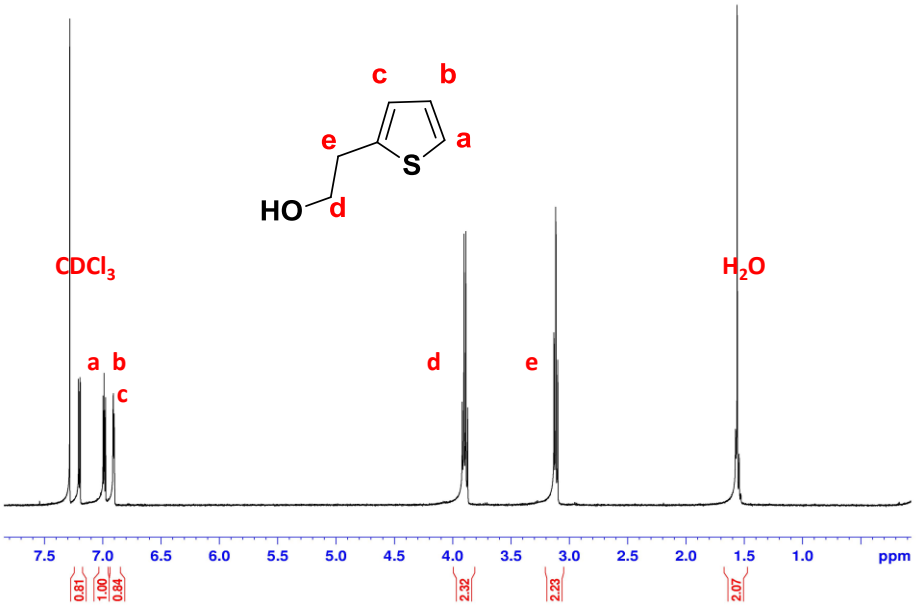

Figure 3.2 ^{1}H-NMR spectrum of 2-(2-thienyl) ethanol. [$CDCl_3$, 25 ^{o}C, 400 MHz]

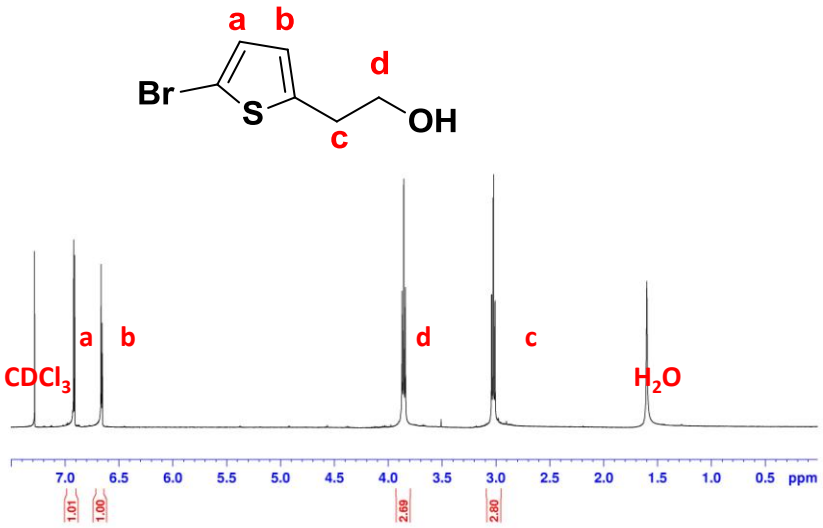

Figure 3.3 ^{1}H-NMR spectrum of M1. [$CDCl_3$, 25 ^{o}C, 400 MHz]

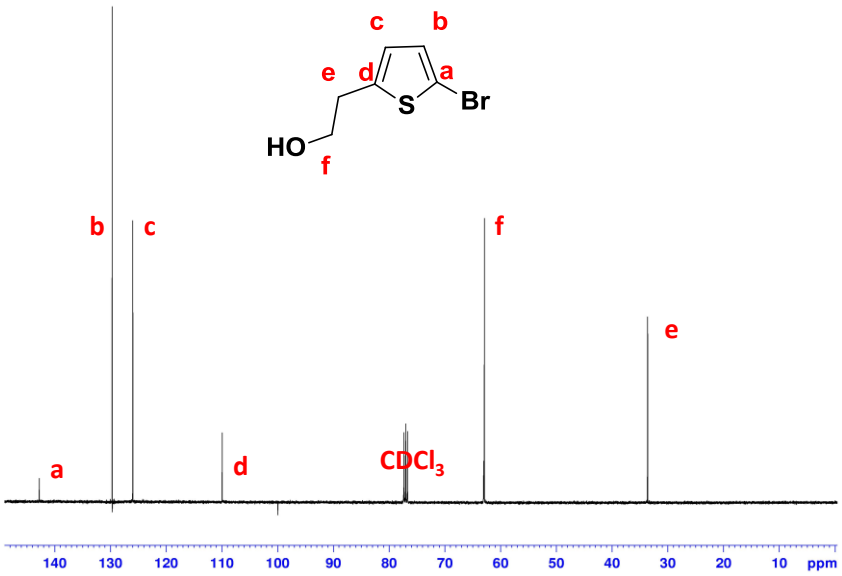

Figure 3.4 ^{13}C-NMR spectrum of M1 [$CDCl_3$, 25 ^{o}C, 100 MHz]

3.1.2 Synthesis of TET1 2,2'-([2,2':5',2'':5'',2'''-quaterthiophene]-5,5'''-diyl)diethanol:

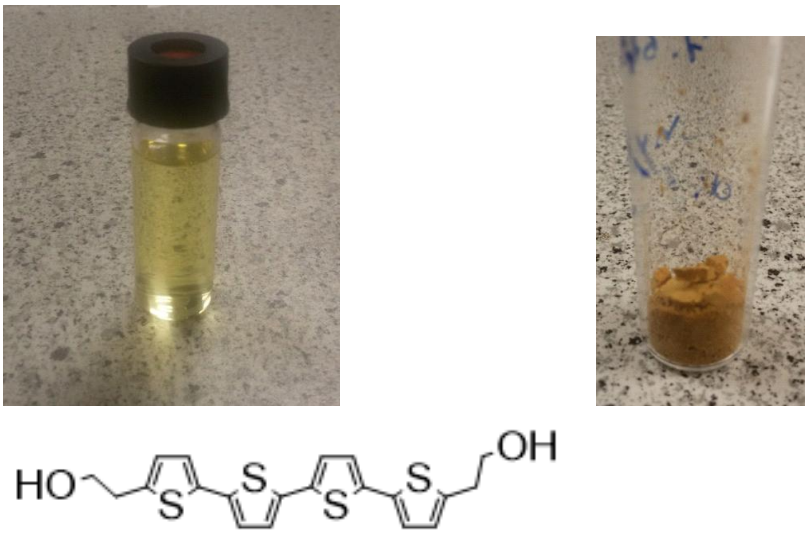

Figure 3.5 TET1 solid state and solution in DCM.

The synthesis of the tetramer and formation of the single C-C bonding between the thiophenes was done by Stille Coupling at high temperature 90^{o}, where Tetrakis(triphenylphosphine)palladium(0) was used as catalyst. The catalytic cycle starts by the oxidative addition to the catalyst which has tetrahedral structure (16 electrons), where Pd(0) is oxidized to Pd(II) forming 18 electrons octahedral complex, by adding the R_1-Br (M1) in cis position, then by cis-trans isomerization, trans R1- Pd – Br is obtained. [85] In the next step transmetallation takes place where the ligand is transferred from Sn atom and connected to the oxidized Pd^{II}, and gives stable bromo-tributlstannane $Sn(butyl)_3Br$ as side product. Then again trans-cis isomerization takes place and the final step happens by the elimination of the product R_1-R_2 which both are in cis position to each other (scheme 3.3). In order to preserve the catalyze Pd(0) not to be oxidized neither with O_2 in air nor dissolved one, the reaction is done in well dried DMF under stream of N_2, and after applying freeze-thaw degassing technique for maximum performance of the catalyst as described in the experimental part (2.3.2).

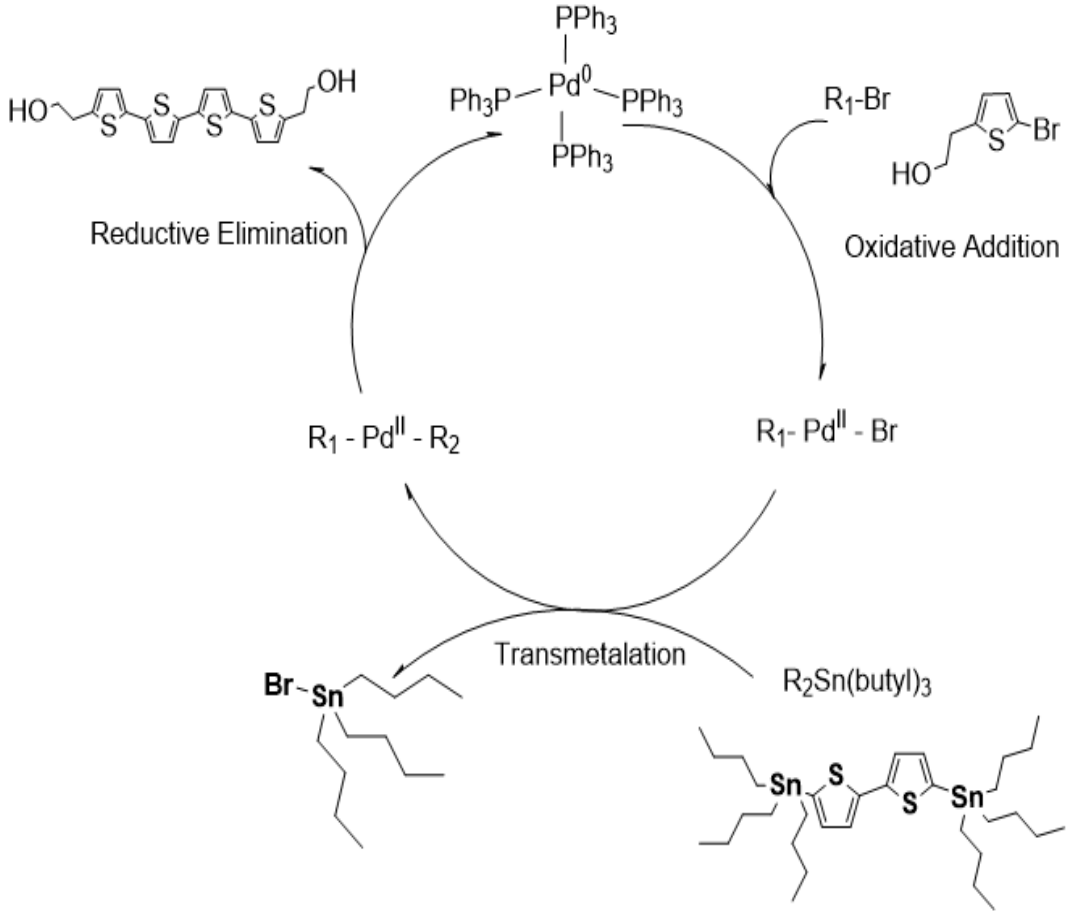

Scheme 3.3 Stille Coupling mechanism for TET1 formation.

The product was characterized by ^{1}H-NMR, ^{13}C-NMR, LC/MS- TOF, UV-VIS, and PL; molar absorptivity and quantum yield were also calculated.

The substrate 5,5'-bis(tributylstannyl)-2,2'-bithiophene, has two positions for reaction therefore requires at least 2 equivalent of the M1; no mono substituted product was obtained, which was controlled by adding extra amount of M1 (2.2 equivalent) and it could be concluded by the comparison between: 5,5'-bis(tributylstannyl)-2,2'-bithiophene ^{1}H-NMR (figure 3.6) where butyl protons in the region (0.9- 1.7 ppm) which considered characteristic are absent from TET1 ^{1}H-NMR spectrum in that particular region. Moreover, ^{13}C-NMR of the TET1 is not showing any extra carbon peaks on the spectrum. The empty area of the spectrum between (0.9 - 1.7 ppm) doesn't only prove the reaction completion to both sides of bithiophene but also the purity of the product from the side product

bromotributlstannane, which has similar butyl characteristic NMR peaks. Figures 3.7 and 3.8.

Similar environment of the aromatic protons caused overlapping and absence of several proton peaks, however the integration shows all the protons.

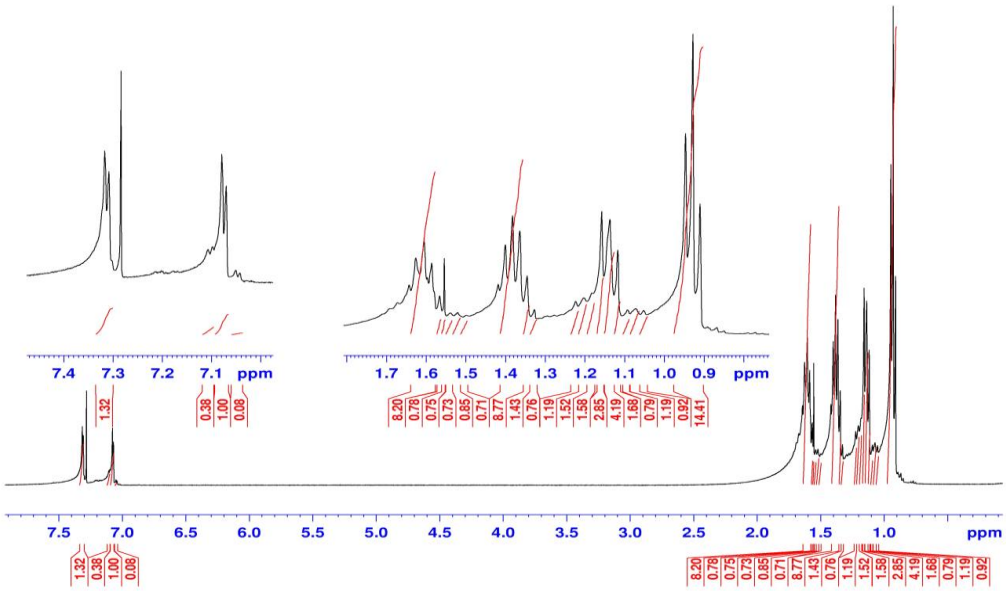

Figure 3.6 ^{1}H-NMR spectrum of 5,5'-bis(tributylstannyl)-2,2'-bithiophene . [$CDCl_3$, 25 ^{o}C, 400 MHz].

DMSO(d_6) was preferred for ^{13}C-NMR because of the very good solubility of TET1 in it comparing to lower solubility in $CDCl_3$ which affected observing the peaks when tested earlier.

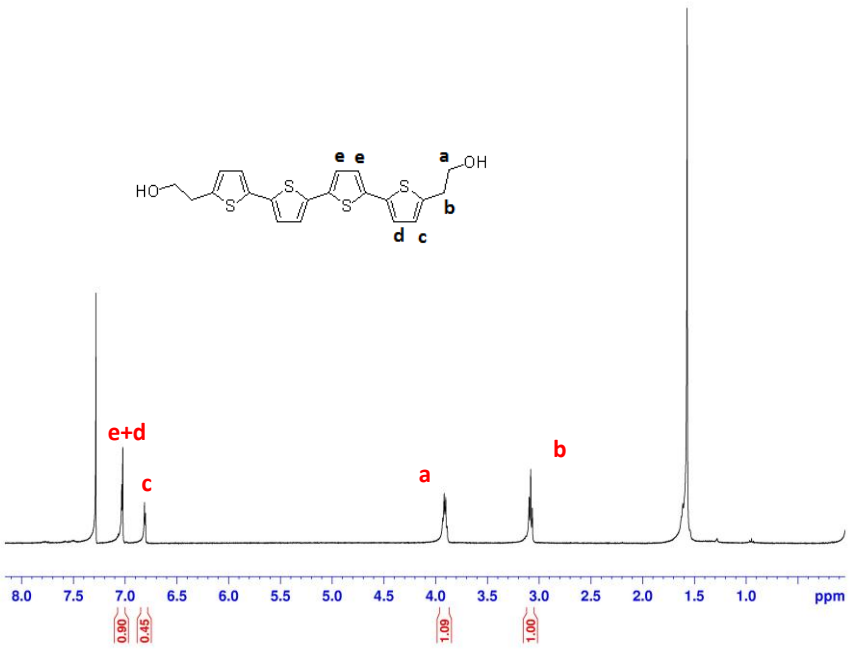

Figure 3.7 ^{1}H-NMR spectrum of TET1. [$CDCl_3$, 25 ^{o}C, 400 MHz].

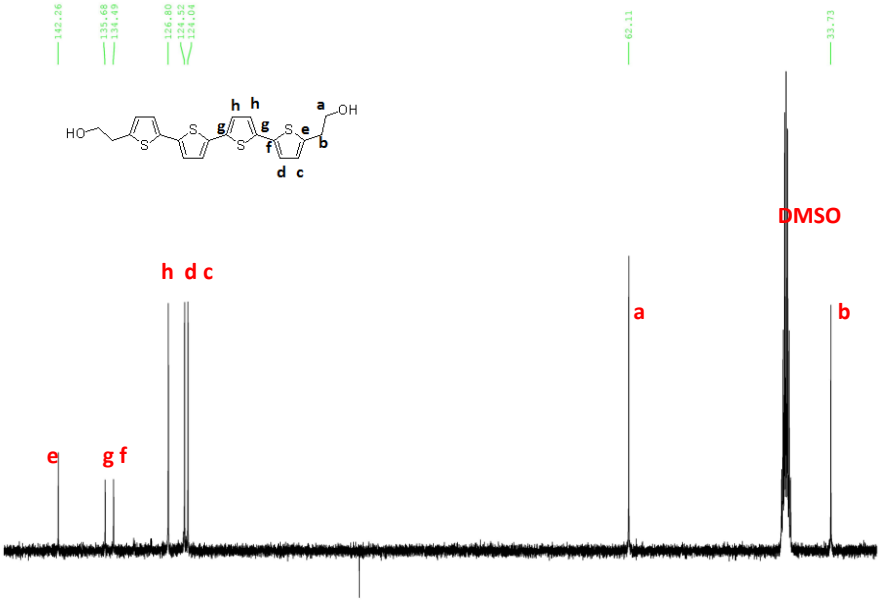

Figure 3.8 ^{13}C-NMR spectrum of TET1. [DMSO(D_6), 25 ^{o}C, 100 MHz].

The product has two hydroxyl groups therefore high polarity is expected and it was seen by TLC's mobile phase and tested with several solvents, where notable solubility was found in higher polar solvents such as THF and DMSO, lower in $CHCl_3$ and DCM, and almost no solubility in nonpolar solvents such as cyclohexane (table 3.1); this character made Stille Coupling an advantage, since the side product bromo-tributlstannane is soluble in cyclohexane and cold ethanol, therefore pure product was obtained by washing with cyclohexane and then precipitating in cold ethanol as described in and can be seen from NMR spectrums supporting the structure and its purity.

Product's solubility:

High solubility	Low-Average Solubility	Not soluble
DMSO, THF, DMF	Cold EtOH, EtOAc, $CHCl_3$, cold MeOH, DCM	Cyclohexane, n-hexane (very low), water

Table 3.1 TET1 solubility.

LC/ MS HRMS TOF was taken and showed the molecular weight of TET1 to be theoretically 418.01841 g/mol^{-1}, when acetonitrile was used as a solvent and the instrument was set for positive ion detection with V_{cap}= 2500 V.
M calculated= 418.01841 m\z, found= 418.01565 m\z, error= 6.9 ppm, (M+1) 419.018 25.5%, (M+2) 420.013 21%, (M+3) 421.114 13% (figure 3.9)

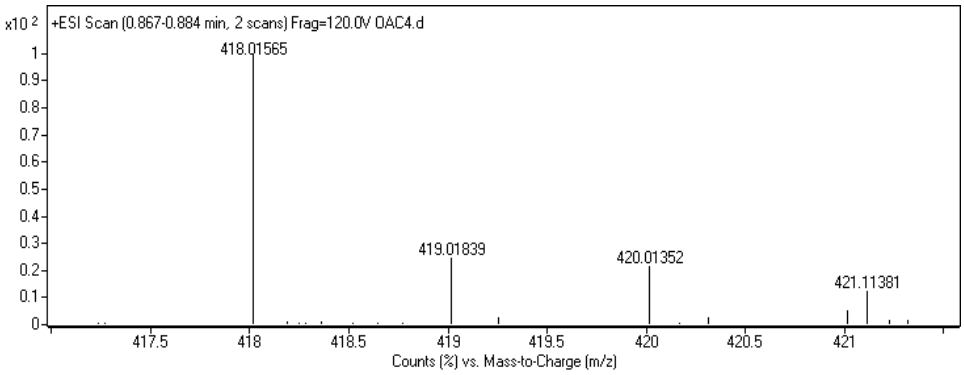

Figure 3.9 Mass spectrum of TET1

3.1.3 Synthesis of P1

In order to attach polyethylene glycol to the tetramer (pegylation) several attempts were considered. According to the structure, copper catalyzed click reaction could have worked by propargylating TET2 and clicking it with azided polyethylene glycol which prepared from bromine-terminated polyethylene glycol. However, the propargylation of TET2 with propargyl bromide in basic medium, where tosyl is good leaving group did not happen and the reaction went to E2 mechanism by the basic catalysis of potassium carbonate, where longer conjugation was preferred by forming ethylene bridges conjugated with the thiophene cycles.

The connection was rather performed by nucleophilic substitution of S_N2 mechanism in basic medium of sodium hydride (scheme 3.4)

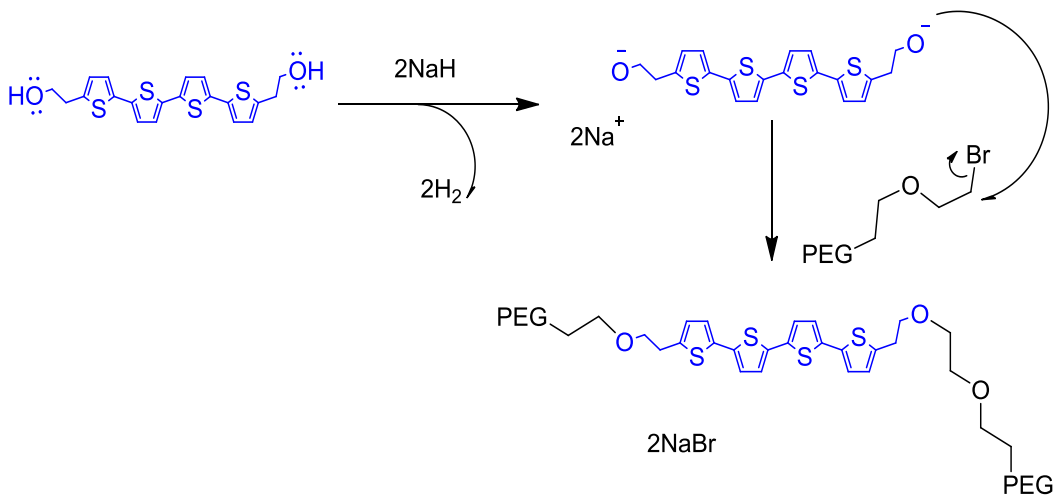

Scheme 3.4 P1 formation mechanism

TET1 was activated by abstracting the acidic protons of alcohol groups in direct reaction by forming hydrogen gas which occurs in cruel conditions; including excess of basic catalysis of sodium hydride in well-dried DMF as aprotic solvent in inert atmosphere of N_2, the order of the reaction is also important; after one hour of the activation, the bromine terminated PEG was added, then the reaction was left for 72 hours. The first confirmation to introducing the PEG into TET1 was by forming water soluble light emitting solution. The water solubility

property was used to purify the product using Sephadex column as described in experimental section.

The characterization was done by ^{1}H-NMR (figure 3.10) which basically shows two groups of peaks, aliphatic protons of polyethylene glycol and shifted aromatic protons. Also brief mass spectroscopy analysis showed the absence of characteristic free bromine peaks (appendix figures A.8, A.9)

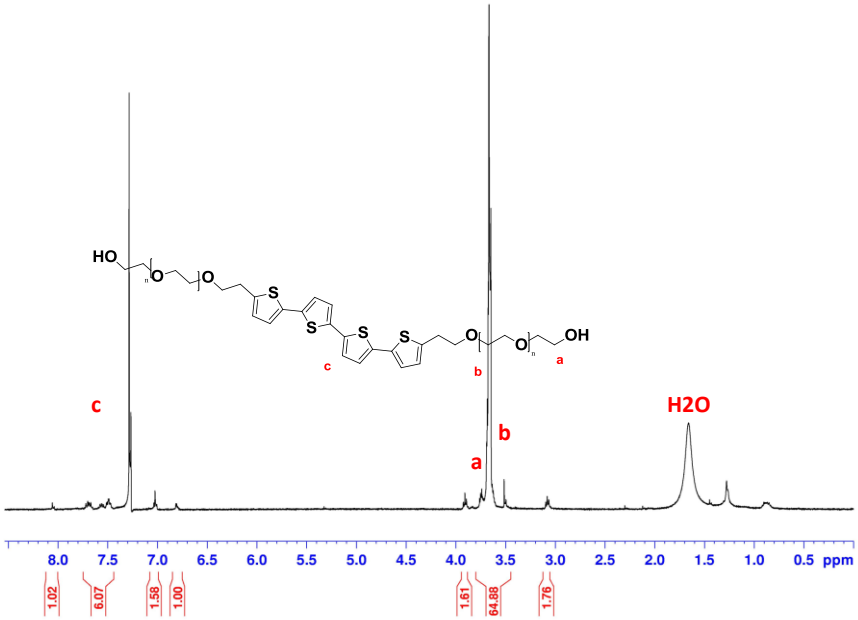

Figure 3.10 P1 ^{1}H-NMR [$CDCl_3$, 25 ^{o}C, 400 Hz]

3.1.4 Synthesis of M2, 2-(2-bromothiophen-3-yl)ethanol:

The mechanism of obtaining M2 is same as M1, both materials have similar polarities (Rf; M2= 0.45, M1= 0.51) and nmr spectrums. The major difference between M1 and M2 is 3TE has two available active positions for reactions (2 and 5), while position 2 is more reactive, still the reaction gives dibromo product 2-(2,5-dibromothiophen-3-yl)ethanol in big amount within the experiment's conditions which affects the yield of M2 and makes it hard to be purified, therefore to be used.

M2 was characterized by ^{1}H-NMR where only two groups of peaks can be recognized in the aromatic region (figure 3.11) which proves the formation and the purity of the product.

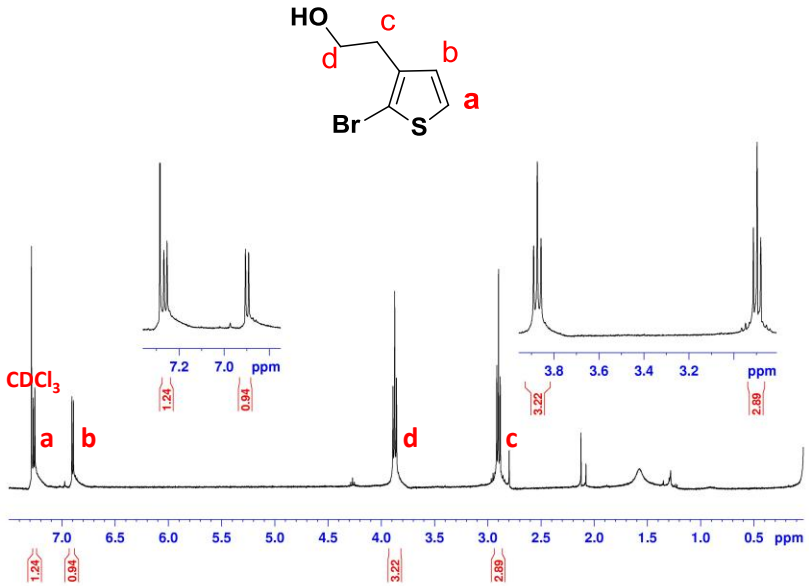

Figure 3.11 M2 ^{1}H-NMR [$CDCl_3$, 25 ^{o}C, 400 Hz]

3.1.5 Synthesis of M3, 2-(5-bromo-2-thienyl)ethyl 4-methylbenzenesulfonate:

After synthesizing M1 as described in the experimental section, it was functionalized with *p*-toluene-sulfonic acid ester as good leaving group. Although there is the possibility of directly functionalizing TET1 with tosyl- group, it was more appropriate to functionalize simple mono hydroxyl structure, which would form one tosylated product easier to be purified, rather than having mono substituted hard to be purified starting from TET1 product if it was to be used.

The leaving group was chosen to be tosyl because the possibility (even if it is small chance) to interfere with the coupling in the next step is much less than bromine which is also widely used as good leaving group.

Tosylation of the M1's hydroxyl was done by introducing the tosyl group of Tosyl chloride (TsCl) in low temperature with basic catalyst to abstract the proton from the hydroxyl group and form the product.

The mechanism is esterification (sulfonic ester formation) with S_N2 substitution mechanism, which depends on the nucleophilicity of hydroxyl group to attack the sulfur forming not stable hydronium structure which will be stabilized by abstracting the acidic proton from the structure using pyridine as a base and forming the product along with pyridinium chloride salt as a side product. Since it is an esterification process with base catalyst then it is balanced reaction. In order to avoid increasing the entropy which might lead to unwanted E2 elimination side product, the reaction is kept at 0^o C. The workup of the reaction is done by extraction in water/ chloroform to exclude the pyridinium chloride water soluble salt, then the process is repeated using acidic water (HCl 1 M) to react with the unreached pyridine and finally basic water of $NaHCO_3$ 1 M is used for neutralization; later, with column chromatography after recovering the polar hydroxylated unreacted starting material (coming second) the product M3 was obtained pure (coming first) with good separation, related to the significant polarity difference between hydroxyl and tosyl groups.

One of the good benefits of tosylation is that the big molecular weight of tosyl group mostly make the product solid, where in this case white solid material was obtained.

The characterization of the product was done by ^{1}H-NMR and ^{13}C-NMR. The structure was confirmed by introducing two characteristic aromatic doublets and one strong singlet of CH_3 of the toluene. Moreover, comparing to M1 ^{1}H-NMR (figure 3.3) the sulfonic group caused to increase the separation between the aliphatic from (3.0- 3.85 ppm) in M1 to (3.1- 4.2 ppm) in M3. No changes were observed on the aromatic protons peaks positions of the thiophene having the environment did not change (Figure 3.12). Same comment can be put on comparing ^{13}C-NMR of M1 and M3 (Figure 3.13).

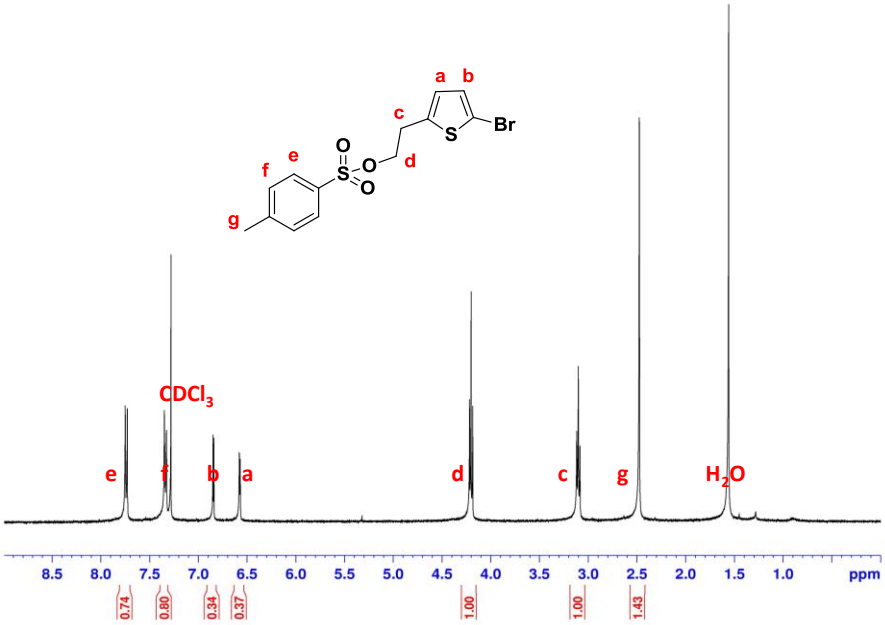

Figure 3.12 ^{1}H-NMR spectrum of M3 [$CDCl_3$, 25 ^{o}C, 400 MHz]

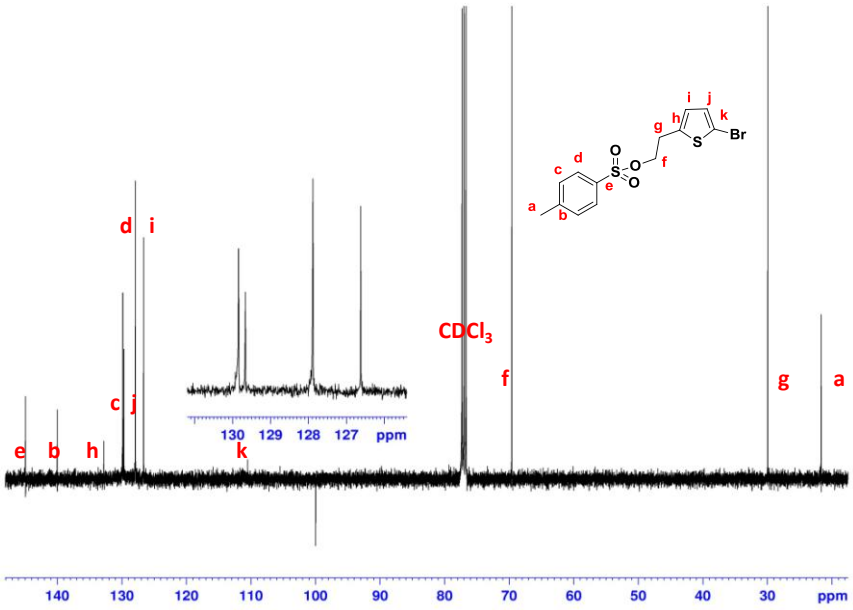

Figure 3.13 ^{13}C-NMR spectrum of M3. [$CDCl_3$, 25 ^{o}C, 100 MHz].

3.1.6 Synthesis of TET2 [2,2':5',2'':5'',2'''-quaterthiophene]-5,5'''-diylbis(ethane-2,1-diyl) bis(4-methylbenzenesulfonate]:

The reaction is Stille Coupling, as discussed above in (3.1.2) with small difference which is changing the solvent (toluene) which is better solvent for reactants with lower polarity and a mixture of two catalysts bis(triphenylphosphine)palladium chloride and tetrakis(triphenylphosphine)palladium $PdCl_2(PPh_3)_2$ and $Pd(PPh_3)_4$.

The product was characterized by ^{1}H-NMR ^{13}C-NMR 2DNMR, LC/MS- TOF, UV-VIS and also PL.

The ^{1}H-NMR confirmed the formation of the molecule by the characteristic two doublets of the benzene cycle that belongs to tosyl- group so as sharp toluenic methyl- singlet in 2.4, moreover crowd aromatic region of thiophenes with the characteristic two triplets at 3.16 ppm and 4.26 ppm (figure 3.14) and ^{13}C-NMR (Figure 3.15).

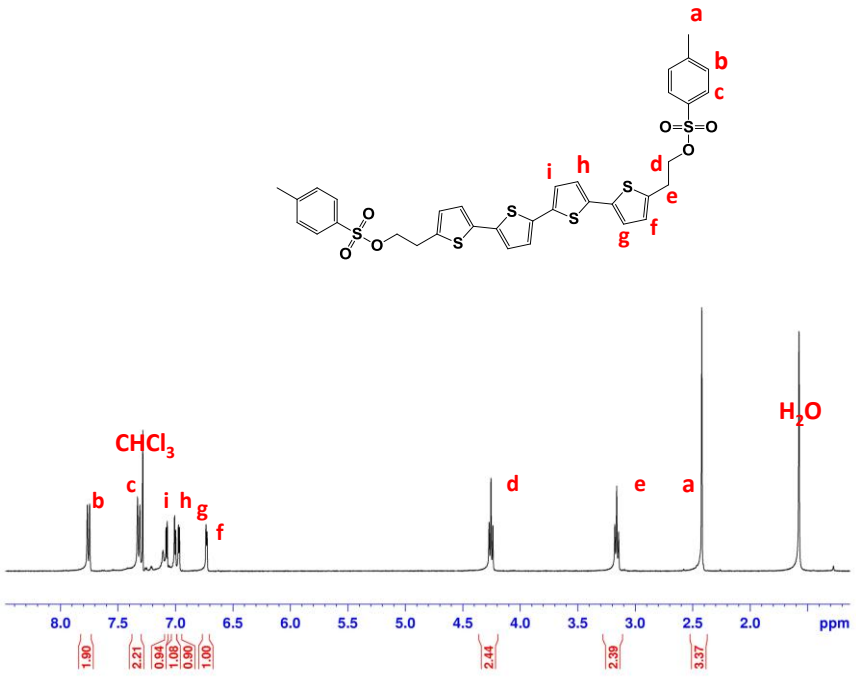

Figure 3.14 ^{1}H-NMR spectrum of TET2. [$CDCl_3$, 25 ^{o}C, 400 MHz].

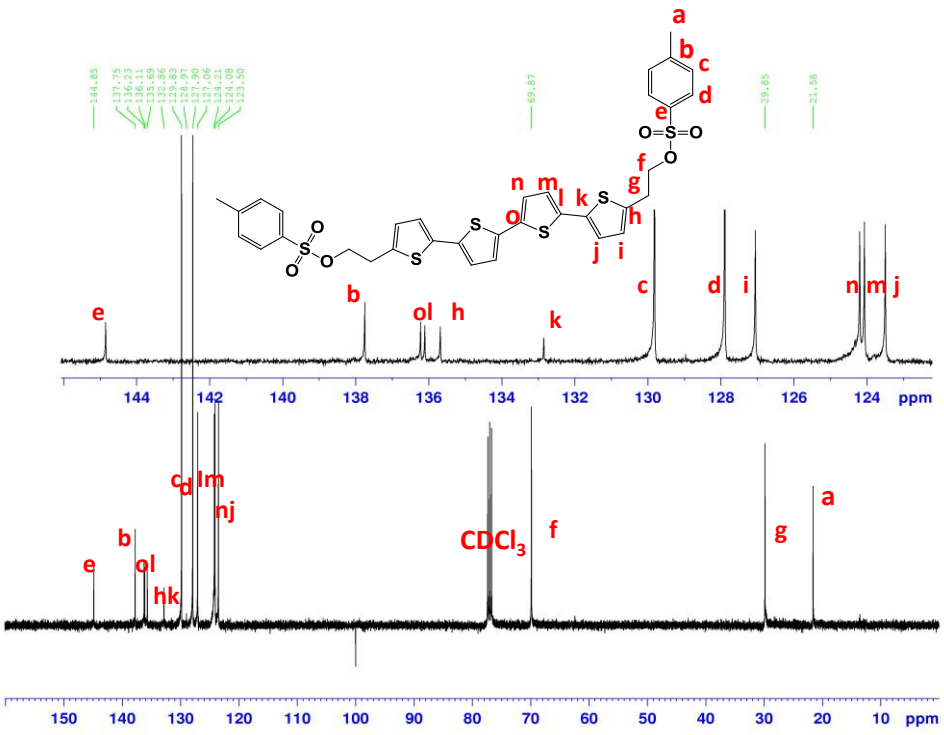

Figure 3.15 ^{13}C-NMR spectrum of TET2. [$CDCl_3$, 25 ^{o}C, 100 MHz].

In order to confirm the many peaks of ^{13}C-NMR and ^{1}H-NMR and matching them with the corresponded atoms, C-H COSY 2D NMR was taken where protons were matched with the related carbon atoms especially for aromatic region (figure 3.16) (see appendix for more focused extended aromatic region)

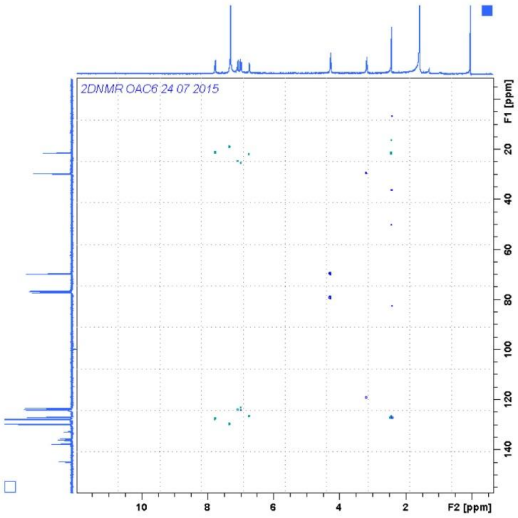

Figure 3.16 TET2 COSY 2DNMR in $CDCl_3$

For mass analysis LC/ MS- HRMS time of flight was used using MeOH as solvent, where Vcap = 3500 V, $[M+H^+]$ calcd for $C_{34}H_{30}O_6S_6$ 727.04 $g.mol^{-1}$, found: 727.04219 $g.mol^{-1}$ error: 2.41ppm. 727.04 (100%), 728.04 (41.34%), 729.04 (34.13%), 730.04 (11.75%) (figure 3.17).

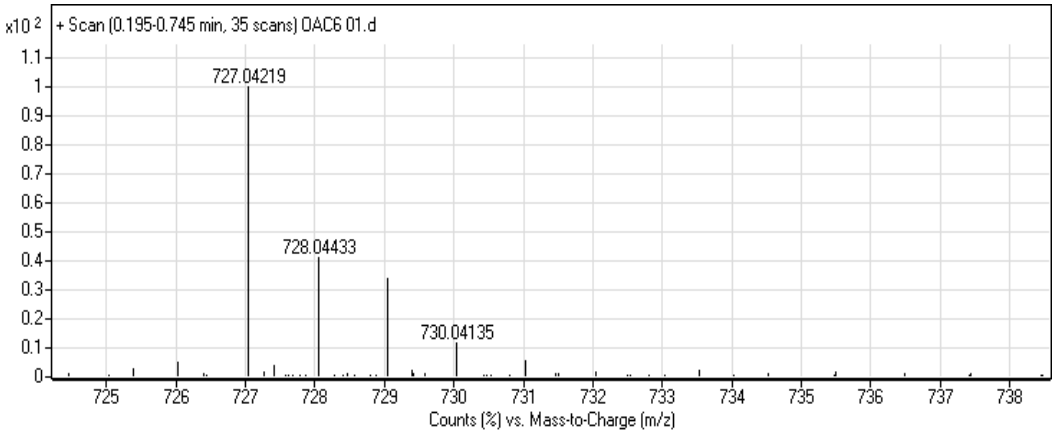

Figure 3.17 MS spectrum of TET2

3.1.7 Synthesis of TET3, 5,5'''-bis(2-azidoethyl)-2,2':5',2'':5'',2'''-quaterthiophene

Having TET2 terminated with tosyl groups makes it easy to be substituted with azide by simple S_N2 mechanism using Sodium azide in aprotic solvent (DMF) with the following mechanism in (scheme 3.5).

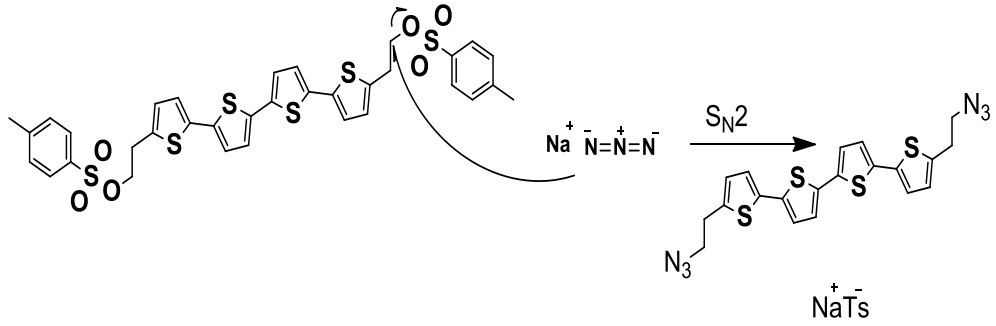

Scheme 3.5 TET3 formation through TET2 azidation.

The product formation can be confirmed in various ways. It was characterized by ^{1}H-NMR, where the two characteristic groups of peaks of tosyl disappeared from ^{1}H-NMR spectrum of TET3 (figure 3.18).

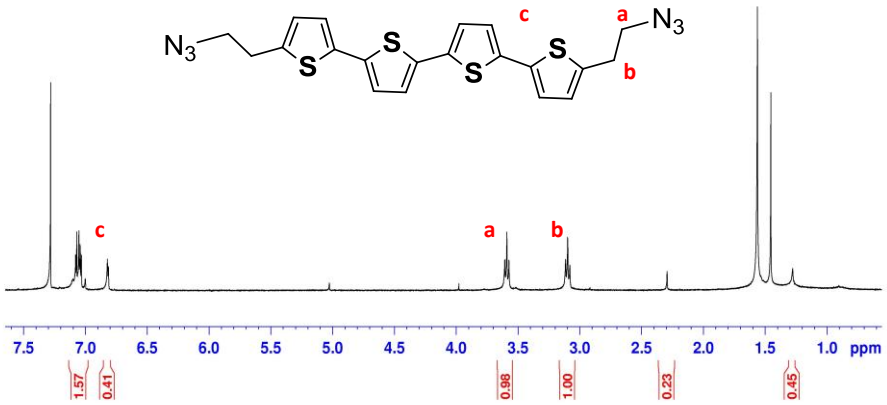

Figure 3.18 ^{1}H-NMR spectrum of TET3. [$CDCl_3$, 25 ^{o}C, 400 MHz].

The existence of the azide peak in particular can be detected by the FT-IR where azide has characteristic strong stretching in 2100 cm^{-1} (figure 3.19).

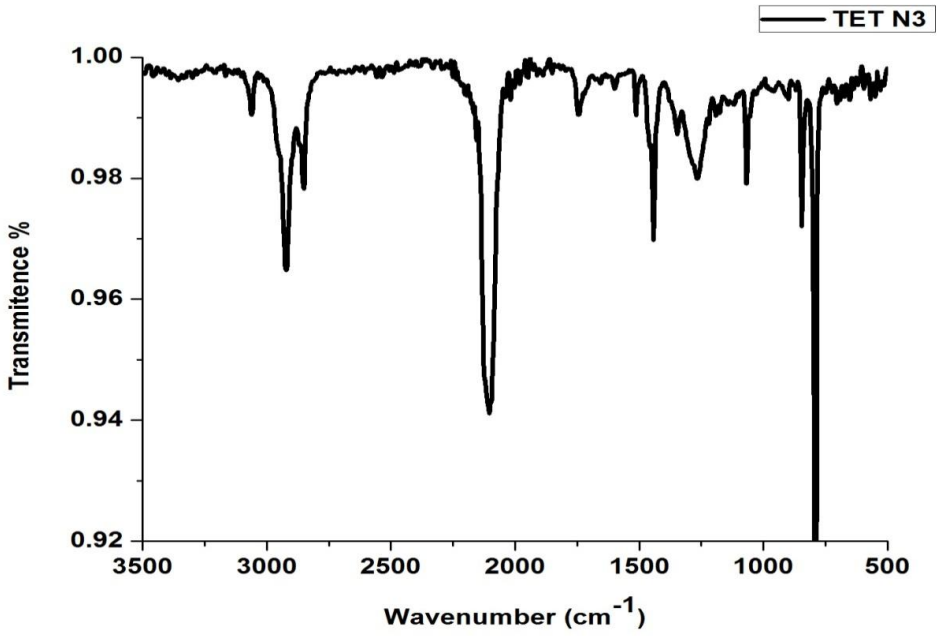

Figure 3.19 TET3, azide stretching.

The azide group has an advantage to be clicked with propargylated moiety or to be degrated to amine group which is better nucleophile than hydroxyl for further reactions.

3.1.8 Photophysical Properties

TET1 and P1 shows light emitting property under UV light source (figure 3.20). In chloroform both TET1 and P1 showed maximum absorbance at 367 nm which can be translated as both functionalities have same auxochromic effect. TET1 has no water solubility even at very low concentration, on the other hand P1 has amphiphilic polyethylene glycol functionalities that increase the affinity toward water to become water soluble; under UV light, P1 showed maximum absorbance at 372 nm, the bathochromic shift is because of solvent effect. (figure 3.21) This solvent effect comes from the smaller energy differences in polar solvents than those in nonpolar solvents. So π^* level in water is lower which allows π to π^* transition to have lower energy which shifts the maximum absorbance to higher wavelength. [86]

Figure 3.20 TET1 (chloroform solution) left, P1 (water) right, under short wave length UV lamp.

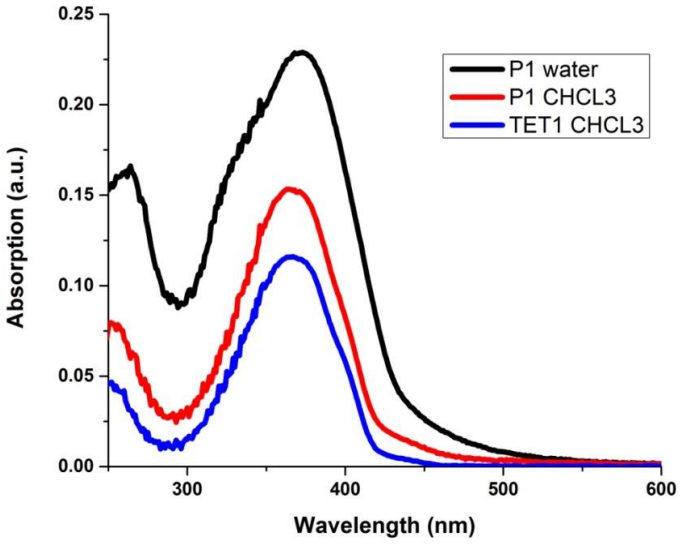

Figure 3.21 UV absorbance of TET1 and P1

At the maximum absorbance, fluorescence was also studied (figure 3.22). It showed same emission wave length in chloroform for both TET1 and P1 (λ_{em}= 445 nm), while P1 showed emission at 455 nm when was excited at 372 nm in water.

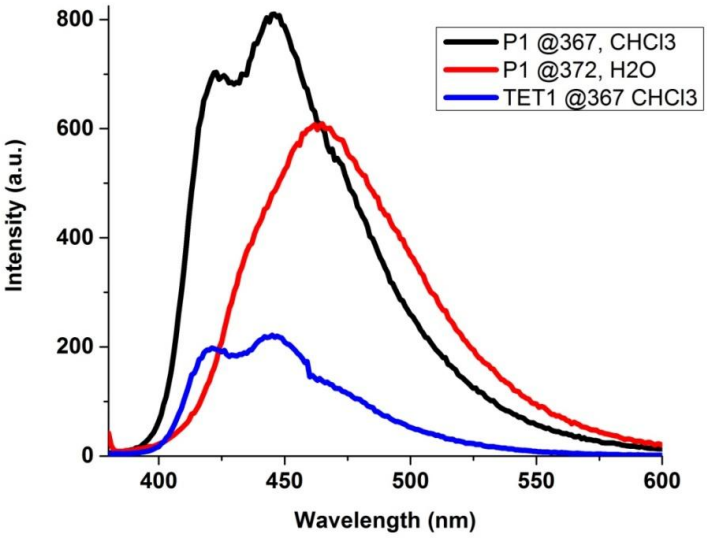

Figure 3.22 PL of TET1 and P1.

TET2 and TET3 showed red shifting when compared to TET1, this red shifting is because of the stronger auxochromic effect for azide and tosyl which enrich the aromatic, however, tosyl and azide have no much difference between each other which can be seen in very close maximum absorbance (TET2 400 nm, TET3 405) (figure 3.23). At the maximum absorbance, photoluminescence was studied and compared (figure 3.24). It showed almost same bright green emission in chloroform for both TET2 and TET3 at wave length (λ_{em}= 490 nm).

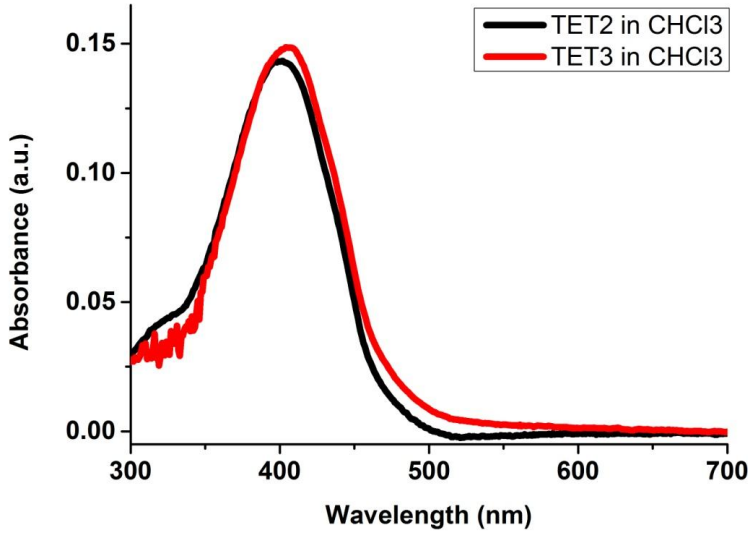

Figure 3.23 UV absorbance comparison for TET2 and TET3

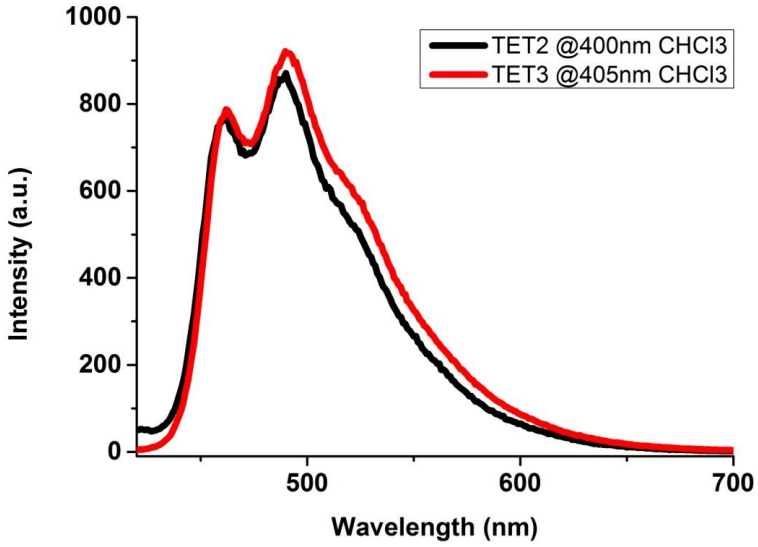

Figure 3.24 TET2 and TET3 PL

Molar absorptivity was measured in THF for TET1 and in water for P1, from Beer–Lambert equation A= ε.c.l. Also quantum yield was calculated for TET1 in THF by procedure mentioned in (2.3.9)

	Solvent	**ε ($cm^{-1}.M^{-1}$)**	**Φ**
TET1	THF	10656	19.81% ± 1.67
P1	Water	22120	-

Table 3.2 Molar absorptivity and quantum yield for TET1 and P1.

3.2 Section 2: Synthesis of Nanoparticles and The Morphological Study:

Three different sets of nanoparticles were synthesized as described in (2.3.8) More thoroughly direct preparation of P1 in water as described in experimental part (2.3.8.3), the maximum solubility in water was checked using the same procedure and was found to be (0.1 $mg.ml^{-1}$).

Series of concentrations was prepared by injecting the stock solution while stirring into dd water where the total volume of the solution prepared to be 10 ml. After preparing the solutions P1 chains would be self-assembled in nanostructures that allow the hydrophobic backbone of the thiophenes to stack and to be surrounded by the long amphiphilic polyethylene glycol chains keeping the hydrophobic thiophenes away from water which is considered the driving force for the nanoparticles formation (scheme 3.6).

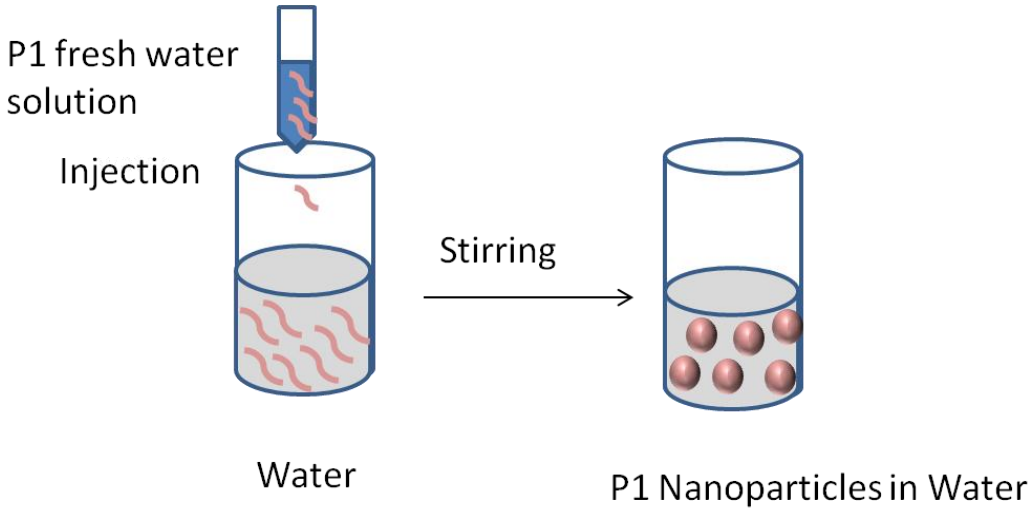

Scheme 3.6 self-assembled P1 NPs in water.

The solutions were characterized first by dynamic light scattering (DLS) to analyze size distribution of the particles by measuring their Brownian Motion (figure 3.25). This showed the optimum concentration among the different set of concentrations to be 0.02 $mg.ml^{-1}$ which gave nanoparticles size of 21 nm with polydispersity index 0.364.

		Diam. (nm)	% Number	Width (nm)
Z-Average (r.nm): 74,80	Peak 1:	21,92	100,0	9,655
PdI: 0,364	Peak 2:	0,000	0,0	0,000
Intercept: 0,463	Peak 3:	0,000	0,0	0,000

Result quality : Good

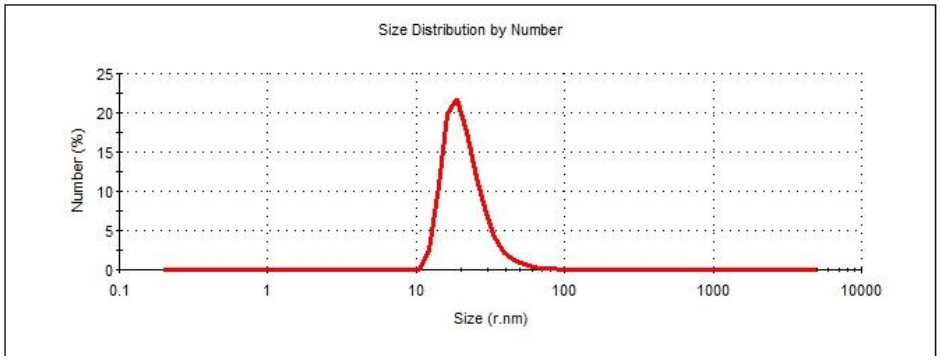

Figure 3.25 DLS of water self-assembled nanoparticles

After DLS analyzation the morphology was studied by SEM microscope which showed nanoparticles with diameter range of 20-37 nm (figure 3.26) Higher concentrations showed bigger particles and aggregations in SEM therefore, 0.02 $mg.ml^{-1}$ was considered.

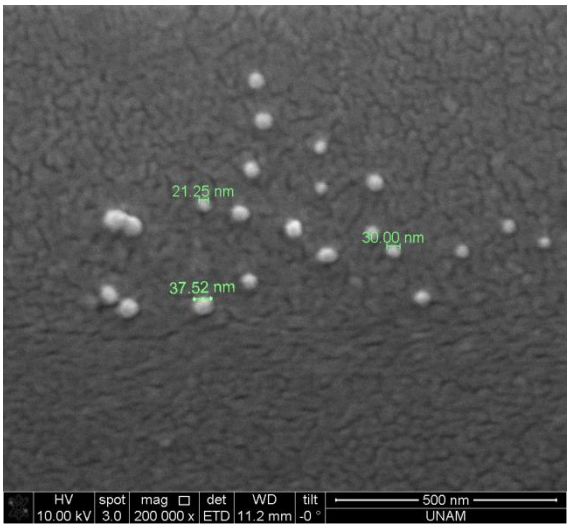

Figure 3.26 SEM of water self-assembled nanoparticles

On another two experiments, P1 was dissolved in THF and injected in water (10 ml) giving concentration of 0.02 $mg.ml^{-1}$, while either stirring for one hour or sonicating for one hour as illustrated in the scheme bellow, (scheme 3.7).

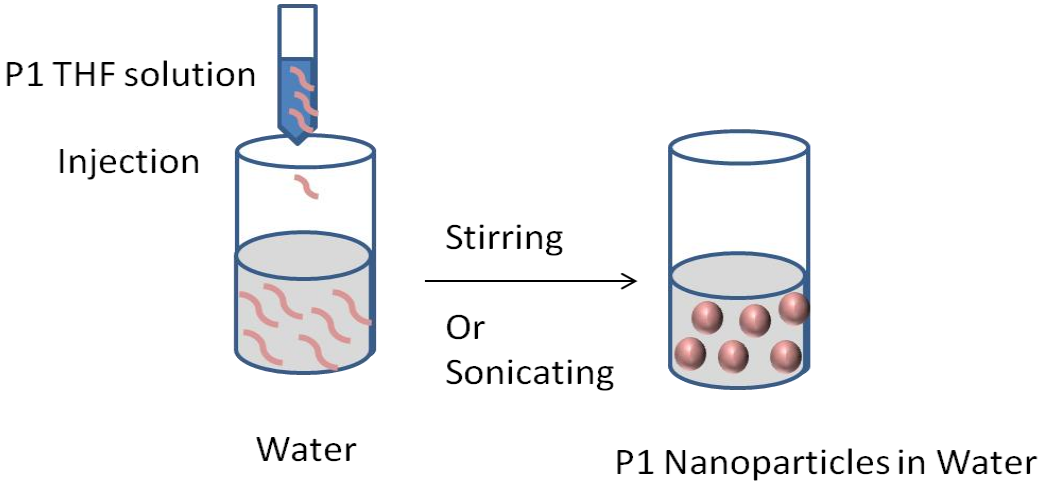

Scheme 3.7 Nanoparticles preparation with reprecipitation method.

This also showed nanoparticles formation in water which was studied by DLS. The results were very close, however, the self-assembled sample gave narrower polydispersity index (PdI) rather than the sonicated sample. The morphology was checked using TEM microscopy which showed rounded nanoparticles with about 30 nm diameters. Sonicated sample: Figures 3.27, 3.28, 3.29. Self-assembled sample: Figures 3.30, 3.31, 3.32.

			Diam. (nm)	% Number	Width (nm)
Z-Average (d.nm):	87,04	Peak 1:	37,26	100,0	12,46
PdI:	0,377	Peak 2:	0,000	0,0	0,000
Intercept:	0,740	Peak 3:	0,000	0,0	0,000

Result quality : Refer to quality report

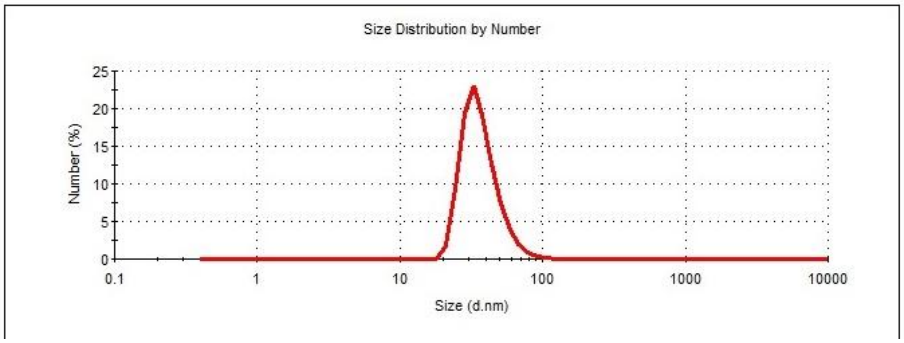

Figure 3.27 Size distribution of P1 NP's by ultrasonication using reprecipitation method in THF.

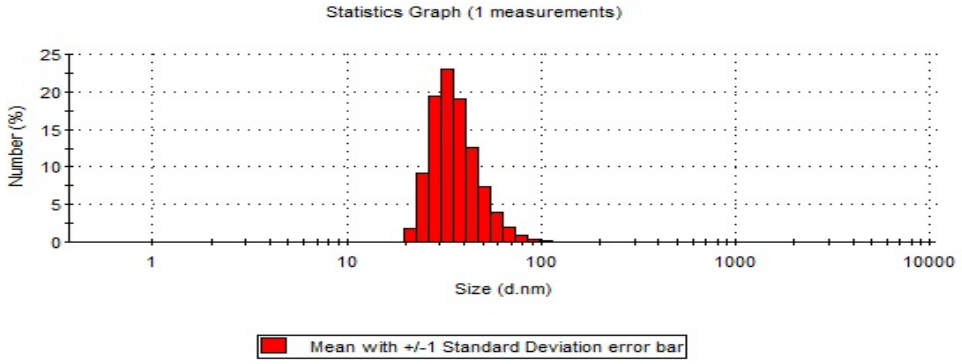

Figure 3.28 Number Deviation of P1 NP's by sonication using reprecipitation method in THF.

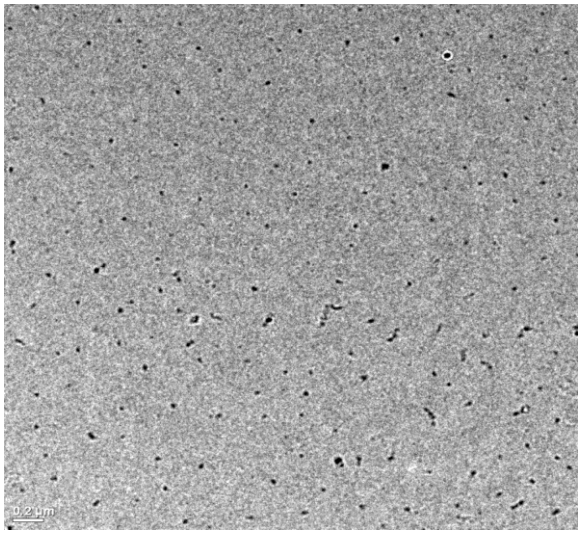

Figure 3.29 TEM image of P1 NP's by sonication using reprecipitation method in THF. Scale 0.2 µm). Particles size (around 40 nm)

			Diam. (nm)	% Number	Width (nm)
Z-Average (d.nm):	58,67	Peak 1:	29,58	100,0	9,411
PdI:	0,201	Peak 2:	0,000	0,0	0,000
Intercept:	0,829	Peak 3:	0,000	0,0	0,000

Result quality : Refer to quality report

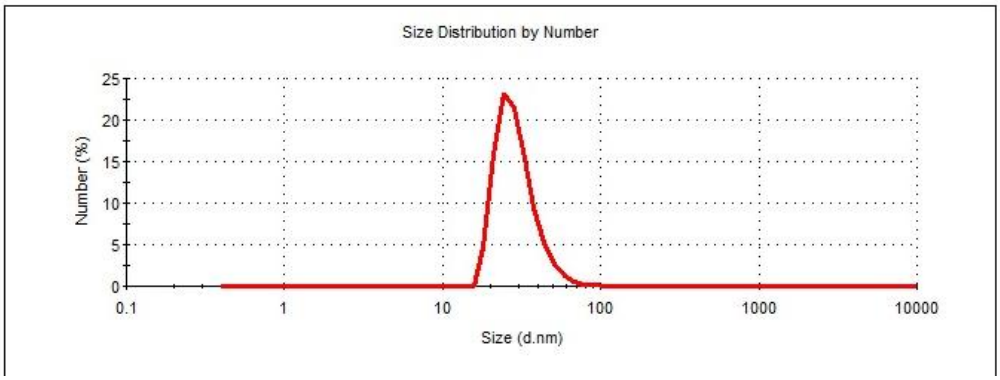

Figure 3.30 Size distribution of P1 self-assembled NP's using reprecipitation method in THF.

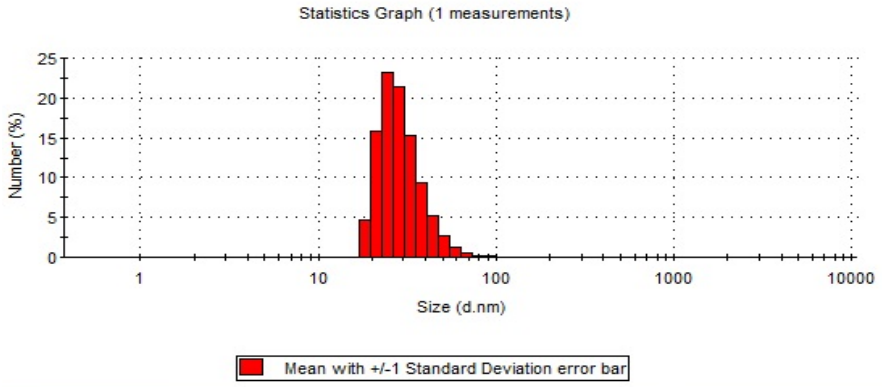

Figure 3.31 Number Deviation of P1 self-assembled NP's using reprecipitation method in THF.

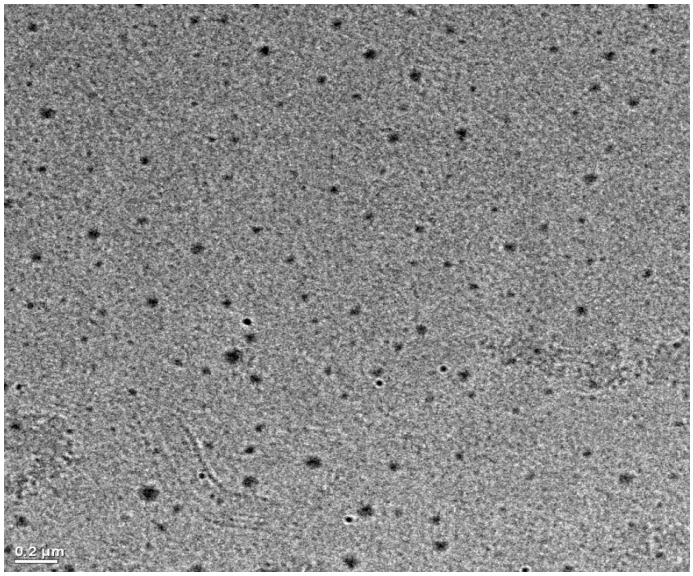

Figure 3.32 TEM image of P1 self-assembled NP's using reprecipitation method in THF. Scale 0.2 µm). Particles size (30-40 nm).

Long term stability:

The self-assembled NP's used sample was stored in room temperature for 5 months and then the morphology was studied again using SEM; the study showed some aggregations but a general stability for both; size (30-40 nm) and formation (round) of the nanoparticles (figure 3.33)

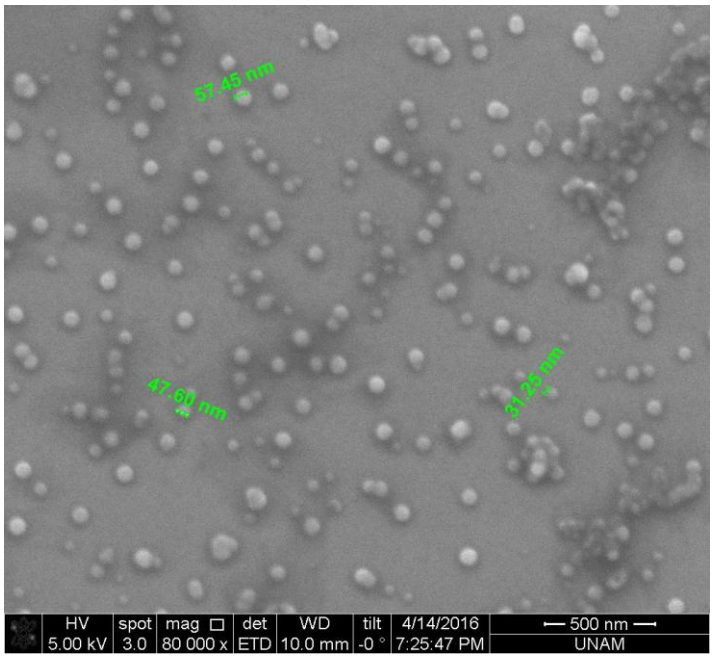

Figure 3.33 SEM of THF-water self-assembled nanoparticles, sample stored for 5 months.

Chapter 4

CONCLUSION

Thiophene based tetramer was synthesized and properly characterized with NMR and MS, Then it was functionalized with polyethylene glycol [1500] forming bifunctional tetramer (PEG- TET -PEG) which was characterized. Photophysical properties were studied and compared for oligomer before and after PEG-ylation.

Nanoparticles were synthesized in water and they were thoroughly studied. Small spherical nanoparticles were obtained (diameter 20 nm), with relatively long term stability.

This macromolecule is predicted to be good candidate for biomedical applications especially as drug carrier system for hydrophobic cancer drugs such as CPT and Doxorubicin. and for other biomedical applications.

On another related study, azide functionalized thiophene based tetramer was synthesized and well characterized. Azide functionality is more reactive functionality comparing to hydroxyl that it can be clicked with propargylated moieties or be degraded to amine which is good nucleophile.

BIBLIOGRAPHY

[1] G. Inzelt, " Conducting Polymers: A New Era in Electrochemistry" *Springer*, Chapter 1: Introduction, pp. 1-6, 2008.

[2] H.-J. Cantow and R. Mulhaupt "Hermann Staudinger and Polymer Research in Freiburg" *Advances in Polymer Science,* vol. 261, pp. 21–38, 2013.

[3] A. M. Saxman, R. Liepins, and M. Aldissi. "Polyacetylene: its synthesis, doping and structure." *Progress in polymer science,* vol. 11, no. 1, pp. 57-89, 1985

[4] The Nobel Prize in Chemistry 1963". *Nobelprize.org.* Nobel Media AB 2014.

[5] A. G. MacDiarmid, "“Synthetic metals”: A novel role for organic polymers (Nobel lecture)." *Angewandte Chemie International Edition,* vol. 40, no. 14, pp. 2581-2590, 2001.

[6] A. D. McNaught and A. Wilkinson , "IUPAC. Compendium of Chemical Terminology, the Gold Book". *Blackwell Scientific Publications, Oxford*, 2nd edition, 1997.

[7] J. Pennakalathil, A. Ozgun, I. Durmaz, R. C. Atalay, D. Tuncel. "pH-Responsive Near-Infrared Emitting Conjugated Polymer Nanoparticles for Cellular Imaging and Controlled-Drug Delivery." *Journal of Polymer Science Part A: Polymer Chemistry,* vol. 53, no. 1, pp. 114-122, 2015.

[8] S. Yang et al "Bandgap calculations for conjugated polymers." *Synthetic Metals,* vol. 141, no. 1, pp. 171-177, 2004.

[9] B. V. Rao, et al "Electronic Circuit Analysis" *Pearson Education,* , Chapter 2, 2012.

[10] C. K. Chiang, et al. "Polyacetylene,(CH) x: n- type and p- type doping and compensation." *Applied Physics Letters*, Vol. 33, No. 1, pp. 18-20, 1978.

[11] P. Atkins, "Physical Chemistry" *Oxford*, 9th edition, Chapter 13, 2010.

[12] R. McNeill, R. Siudak, J. H. Wardlaw, D. E. Weiss "Electronic conduction in polymers. I. The chemical structure of polypyrrole." *Australian Journal of Chemistry*, vol. 16, no. 6, pp. 1056-1075, 1963.

[13] H. S. Nalwa, "Hand Book of Organic Conductive Molecules and Polymers" *Wiley*, Vol. 2, Chapter 4, (1997).

[14] Schatz, J., "Product Subclass 1: Thiophenes" *Science of Synthesis*, 9, pp 287. 2001.

[15] Hou, X. -L.; Peng, X. -S.; Yeung, K. -S.; Wong, H. N. C., 9.9.5 Furans (Update 2011) *Science of Synthesis Knowledge Updates*, 2, pp 261. 2011.

[16] T. Eicher, S. Hauptmann, A. Speicher, "The Chemistry of Heterocycles: Structure, Reactions, Syntheses, and Applications" *Wiley*, 2nd Edition, Chapter 5, 2004.

[17] A. F. Diaz and K. K. Kanazawa and G. P. Gardini. "Electrochemical polymerization of pyrrole." *Journal of the Chemical Society, Chemical Communications*, vol. 14, pp. 635-636, 1979.

[18] A. Sharifi-viand et al. "Determination of fractal rough surface of polypyrrole film: AFM and electrochemical analysis." *Synthetic Metals* vol. 191, pp. 104-112. 2014.

[19] A. Merz, F. Ellinger "Convenient synthesis of α-terthienyl and α-quinquethienyl via a Friedel-Crafts route." *Synthesis*, vol. 1991, no. 06, pp. 462-464, 1991.

[20] D. A. Schluter, C. Hawker, J. Sakamoto , "Synthesis of Polymers: New Structures and Methods" *Wiley*, Chapter 7, 2012.

[21] Y. Kiso, K. Yamamoto, K. Tamao, M. Kumada "Asymmetric homogeneous hydrosilylation with chiral phosphine-palladium complexes." *Journal of the American Chemical Society*, vol. 94, no. 12, pp. 4374–4376, 1972.

[22] The Nobel Prize in Chemistry 2010". *Nobelprize.org.* Nobel Media AB 2014. Web. <http://www.nobelprize.org/nobel_prizes/chemistry/laureates/2010/>

[23] https://en.wikipedia.org/wiki/John_Kenneth_Stille

[24] Akira Suzuki "Nobel Lecture: Cross-coupling Reactions of Organoboranes: An Easy Way for C-C Bonding". *Nobelprize.org.* Nobel Media AB 2014.

[25] Richard F. Heck "Nobel Lecture: Palladium Reactions for Organic Syntheses". *Nobelprize.org.* Nobel Media AB 2014.

[26] J. K. Stille "The palladium- catalyzed cross- coupling reactions of organotin reagents with organic electrophiles [new synthetic methods (58)]."*Angewandte Chemie International Edition in English,* vol. 25, no. 6, pp. 508-524, 1986.

[27] Ei-ichi Negishi "Nobel Lecture: Magical Power of Transition Metals: Past, Present, and Future". *Nobelprize.org.* Nobel Media AB 2014.

[28] D. C. Ebner "*Development and applications of the palladium-catalyzed enantioselective oxidation of secondary alcohols.* Dissertation" (Ph.D.), *California Institute of Technology*. Introduction to Enantioselective Oxidation Chemistry, Chapter 1, 2009.

[29] C. Barnard "Palladium-catalysed C–C coupling: Then and now."*Platinum Metals Review,* vol. 52, no. 1, pp. 38-45, 2008.

[30] J. T. Chen and C. S. Hsu "Conjugated polymer nanostructures for organic solar cell applications." *Polymer Chemistry,* vol. 2, no. 12, pp. 2707-2722, 2011.

[31] A. Islam, et al. "Enhanced Photovoltaic Performances of Dye-Sensitized Solar Cells by Co-Sensitization of Benzothiadiazole and Squaraine-Based Dyes." *ACS applied materials & interfaces,* vol. 8, no. 7, 4616-4623, 2016.

[32] S. H. Hwang, C. N. Moorefield and G. R. Newkome "Dendritic macromolecules for organic light-emitting diodes." *Chemical Society Reviews, vol.* 37, no. 11, pp. 2543-2557, 2008.

[33] J. Zaumseil and H. Sirringhaus "Electron and ambipolar transport in organic field-effect transistors." *Chemical reviews,* vol. 107, no. 4, pp. 1296-1323, 2007.

[34] Z. Chen, et al "Sensitive Conjugated-Polymer-Based Fluorescent ATP Probes and Their Application in Cell Imaging." *ACS applied materials & interfaces,* vol. 8, no. 6, pp. 3567-3574, 2015.

[35] S. Kolemen, et al. "Intracellular Modulation of Excited- State Dynamics in a Chromophore Dyad: Differential Enhancement of Photocytotoxicity Targeting Cancer Cells." *Angewandte Chemie,* vol. 127, no. 18, pp. 5430-5434, 2015.

[36] Z. He, H. Wu and Y. Cao "Recent advances in polymer solar cells: realization of high device performance by incorporating water/alcohol- soluble conjugated polymers as electrode buffer layer." *Advanced Materials, vol.* 26, no. 7, pp. 1006-1024, 2014.

[37] X. Feng, et al. "Water-soluble fluorescent conjugated polymers and their interactions with biomacromolecules for sensitive biosensors." *Chemical Society Reviews,* vol. 39, no. 7, pp. 2411-2419, 2010.

[38] A. O. Patil, et al. "Water soluble conducting polymers." *Journal of the American Chemical Society,* vol. 109, no. 6, pp. 1858-1859, 1987.

[39] R. Rulkens, M. Schulze, and G. Wegner. "Rigid- rod polyelectrolytes: synthesis of sulfonated poly (p- phenylene) s." *Macromolecular rapid communications,* vol. 15, no. 9, pp. 669-676, 1994.

[40] M. R. Pinto, K. S. Schanze, "Conjugated Polyelectrolytes: Synthesis and Applications" *Synthesis* 2002, No. 9, pp. 1293-1309.

[41] A. Åslund, et al. "Novel pentameric thiophene derivatives for in vitro and in vivo optical imaging of a plethora of protein aggregates in cerebral amyloidoses." *ACS chemical biology,* vol. 4, no. 8, pp. 673-684, 2009.

[42] H. A. Ho, et al. "Colorimetric and fluorometric detection of nucleic acids using cationic polythiophene derivatives." *Angewandte Chemie,* vol. 114, no. 9, pp. 1618-1621, 2002.

[43] A. Gutacker, et al. "All-conjugated polyelectrolyte block copolymers."*Journal of Materials Chemistry,* vol. 20, no. 8, pp. 1423–1430, 2010.

[44] C. Xue, F. T. Luo, and H. Liu. "Post-polymerization functionalization approach for highly water-soluble well-defined regioregular head-to-tail glycopolythiophenes." *Macromolecules,* vol. 40 no. 19, pp. 6863-6870, 2007.

[45] P. van Rijn, et al. "Self-assembly behaviour of conjugated terthiophene surfactants in water." *New Journal of Chemistry,* vol. 35, no. 3, pp. 558-567, 2011.

[46] Q. Chen, et al. "Fluorescent Conjugated Polyfluorene with Pendant Lactopyranosyl Ligands for Studies of Ca2+-Mediated Carbohydrate− Carbohydrate Interaction." *Biomacromolecules,* vol. 11, no. 1, pp. 13-19, 2009.

[47] P. N. Taylor, et al. "Insulated molecular wires: synthesis of conjugated polyrotaxanes by Suzuki coupling in water." *Angewandte Chemie International Edition,* vol. 39, no. 19, pp. 3456-3460, 2000.

[48] D. Tuncel, M. Artar, and S. B. Hanay, "The effect of cucurbit [n] uril on the solubility, morphology, and the photophysical properties of nonionic conjugated polymers in an aqueous medium" *Journal of Polymer Science Part A: Polymer Chemistry*, vol. *48, no.* 21, pp. 4894-4899, 2010.

[49] J. Pennakalathil, D. Tuncel, et al. "Red emitting, cucurbituril-capped, pH-responsive conjugated oligomer-based nanoparticles for drug delivery and cellular imaging." *Biomacromolecules,* vol. 15, no. 9, pp. 3366-3374, 2014.

[50] B. de Boer, et al. "Amphiphilic, regioregular polythiophenes."*Macromolecules,* vol. 35, no. 18, pp. 6883-6892, 2002.

[51] L. Jiang, R. C. Hughes, D. Y. Sasaki "Supramolecular assembly of a quaterthiophene surfactant." *Chemical communications, vol.* 8, pp. 1028-1029, 2004

[52] H. L. Zhang, et al. "Fluorogenic probing of specific recognitions between sugar ligands and glycoprotein receptors on cancer cells by an economic graphene nanocomposite." *Advanced Materials,* vol. 25, no. 30, pp. 4097-4101, 2013.

[53] K. Sakamoto, et al. "Preparation and Properties of Rotaxanes Formed by Dimethyl-β-cyclodextrin and Oligo (thiophene) s with β-Cyclodextrin Stoppers."*The Journal of organic chemistry* 72.2 (2007): 459-465.

[54] K. I. Assaf, and M. N. Werner "Cucurbiturils: from synthesis to high-affinity binding and catalysis." *Chemical Society Reviews*, vol. 44, no. 2, pp. 394-418, 2015.

[55] A. Harada, et al. "Polymeric rotaxanes." *Chemical reviews,* vol. 109, no. 11 , pp. 5974-6023, 2009.

[56] M. Delbianco, et al. "Carbohydrates in supramolecular chemistry."*Chemical reviews,* vol. 116, no. 4, pp. 1693-1752, 2015.

[57] S. Gürbüz, M. Idris, and D. Tuncel. "Cucurbituril-based supramolecular engineered nanostructured materials." *Organic & biomolecular chemistry,* vol. 13, no. 2, pp. 330-347, 2015.

[58] L. Feng, et al. "Conjugated polymer nanoparticles: preparation, properties, functionalization and biological applications." *Chemical Society Reviews*, vol. 42, no. 16, pp. 6620-6633, 2013.

[59] A. B. Chinen, et al. "Nanoparticle probes for the detection of cancer biomarkers, cells, and tissues by fluorescence." *Chemical Reviews*, vol. 115, no. 19, pp. 10530-10574, 2015.

[60] A. Kaeser, and A. PHJ Schenning. "Fluorescent Nanoparticles Based on Self- Assembled π- Conjugated Systems." *Advanced Materials, vol.* 22 no. 28, pp. 2985-2997, 2010.

[61] L. Kai, and B. Liu. "Polymer encapsulated conjugated polymer nanoparticles for fluorescence bioimaging." *Journal of Materials Chemistry,* vol. 22, no. 4, pp. 1257-1264, 2012.

[62] J. Pecher and S. Mecking. "Nanoparticles of conjugated polymers." *Chemical reviews,* vol. 110, no. 10, pp. 6260-6279, 2010.

[63] C. Wu , C. Szymanski, and J. McNeill. "Preparation and encapsulation of highly fluorescent conjugated polymer nanoparticles."*Langmuir*, vol. 22, no. 7, pp. 2956-2960, 2006.

[64] D. Chandler, "Interfaces and the driving force of hydrophobic assembly."*Nature* vol. 437, no. 7059, pp. 640-647, 2005.

[65] D. Tuncel, and H. V. Demir. "Conjugated polymer nanoparticles."*Nanoscale*, vol. 2, no. 4, pp. 484-494, 2010.

[66] P. Liu, et al. "Red-Emitting DPSB-Based Conjugated Polymer Nanoparticles with High Two-Photon Brightness for Cell Membrane Imaging."*ACS applied materials & interfaces*, vol. 7, no. 12, pp. 6754-6763, 2015.

[67] P. Howes, et al. "Phospholipid encapsulated semiconducting polymer nanoparticles: their use in cell imaging and protein attachment." *Journal of the American Chemical Society*, vol. 132. no. 11, pp. 3989-3996, 2010.

[68] Li. Kai, et al. "Generic Strategy of Preparing Fluorescent Conjugated- Polymer- Loaded Poly (DL- lactide- co- Glycolide) Nanoparticles for Targeted Cell Imaging."*Advanced Functional Materials*, vol. 19, no. 22, pp. 3535-3542, 2009.

[69] K-Y. Pu and B. Liu. "Fluorescent conjugated polyelectrolytes for bioimaging." *Advanced Functional Materials*, vol. 21, no. 18 pp. 3408-3423, 2011.

[70] Q. Wang, et al. "Synthesis of water soluble, biodegradable, and electroactive polysaccharide crosslinker with aldehyde and carboxylic groups for biomedical applications." *Macromolecular bioscience*, vol. 11, no. 3, pp. 362-372, 2011.

[71] T. Rivers, T. W. Hudson, and C. E. Schmidt. "Synthesis of a novel, biodegradable electrically conducting polymer for biomedical applications." *Advanced Functional Materials*, vol. 12, no.1, pp. 33-37, 2002.

[72] N. KE. Guimard, J. L. Sessler, and C. E. Schmidt. "Toward a biocompatible and biodegradable copolymer incorporating electroactive oligothiophene units." *Macromolecules,* vol. 42, no. 2, pp. 502-511, 2008.

[73] B. Guo, L. Glavas, and A-C. Albertsson. "Biodegradable and electrically conducting polymers for biomedical applications." *Progress in polymer science* vol. 38, no. 9, pp. 1263-1286, 2013.

[74] H. Tang, et al. "Synthesis of amphiphilic polythiophene for cell imaging and monitoring the cellular distribution of a cisplatin anticancer drug." *Small,* vol. 7, no. 10, pp. 1464-1470, 2011.

[75] O. Gezici, et al. "Dual functionality of conjugated polymer nanoparticles as an anticancer drug carrier and a fluorescent probe for cell imaging." *RSC Advances* vol. 4, no. 3, pp. 1302-1309, 2014.

[76] L. Lu, et al. "Biocidal activity of a light-absorbing fluorescent conjugated polyelectrolyte." *Langmuir* vol. 21 no. 22, pp. 10154-10159, 2005.

[77] B. Wang, et al. "Synthesis of a new conjugated polymer for cell membrane imaging by using an intracellular targeting strategy." *Polymer Chemistry* vol. 4, no. 20, pp. 5212-5215, 2013.

[78] H. Lodish, A. Berk, SL Zipursky, et al. "Molecular Cell Biology" 4th edition. *New York: W. H. Freeman*; Section 12.3, The Role of Topoisomerases in DNA Replication, 2000.

[79] J. L. Nitiss, "Targeting DNA Topoisomerase II in Cancer Chemotherapy."*Nature reviews. Cancer* vol. 9, no. 5, pp. 338–350, 2009.

[80] R. Hardman "A toxicologic review of quantum dots: toxicity depends on physicochemical and environmental factors." *Environmental health perspectives*, vol. 114, pp. 165-172, 2006.

[81] I. López-Duarte, et al. "Thiophene-based dyes for probing membranes."*Organic & biomolecular chemistry* vol. 13, issue. 12, pp. 3792-3802, 2015.

[82] S. T, DeKosky and M. Kenneth "Looking backward to move forward: early detection of neurodegenerative disorders." *Science* vol. 302, no. 5646, pp. 830-834, 2003.

[83] A. Herland, et al. "Synthesis of a regioregular zwitterionic conjugated oligoelectrolyte, usable as an optical probe for detection of amyloid fibril formation at acidic pH." *Journal of the American Chemical Society* vol.127, issue. 7, pp. 2317-2323, 2005.

[84] T. Erdem, et al. "Stable and efficient colour enrichment powders of nonpolar nanocrystals in LiCl." *Nanoscale* vol. 7, issue. 42 pp. 17611-17616, 2015.

[85] R. H. Crabtree, The Organometallic Chemistry of the Transition Metals, John Wiley & Sons, sixth edition, Chapter 6, 2013.

[86] J. W. Robinson, E. M. Skelly Frame, G. M. Frame II, Undergraduate Instrumental Analysis, , CRC Press, Sixth Edition, Chapter 5, 2004.

APPENDIX A

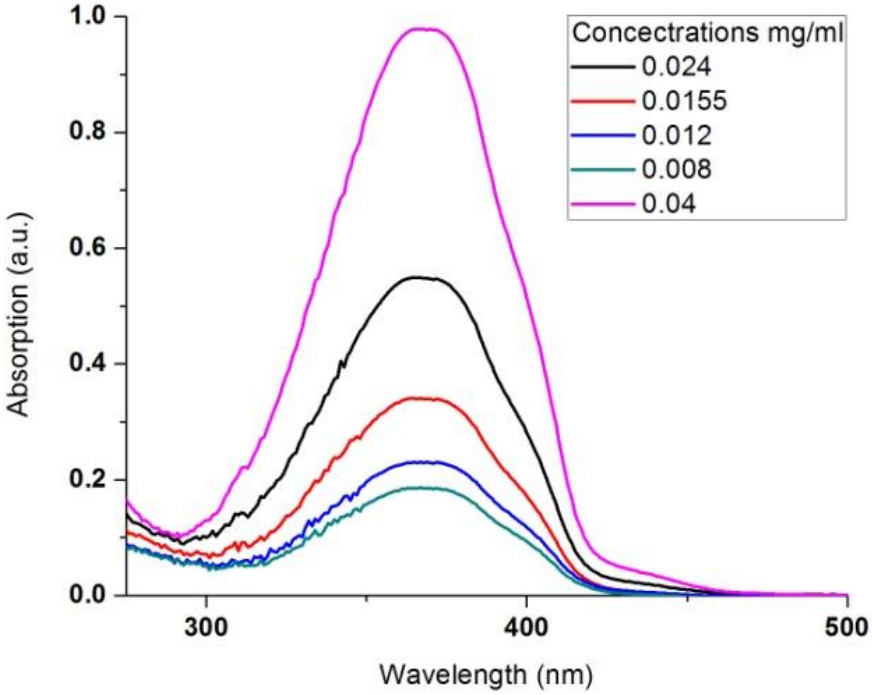

Figure A.1 TET1 UV absorbance series for Molar absorptivity.

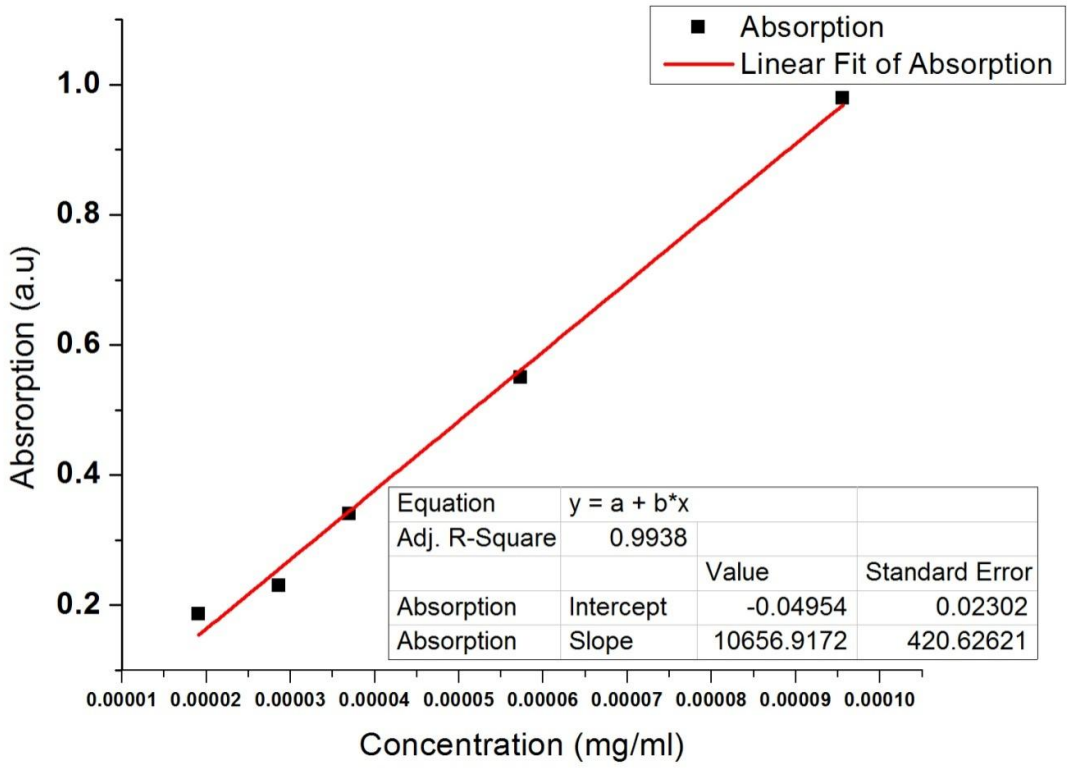

Figure A.2 TET1 molar absorptivity in THF.

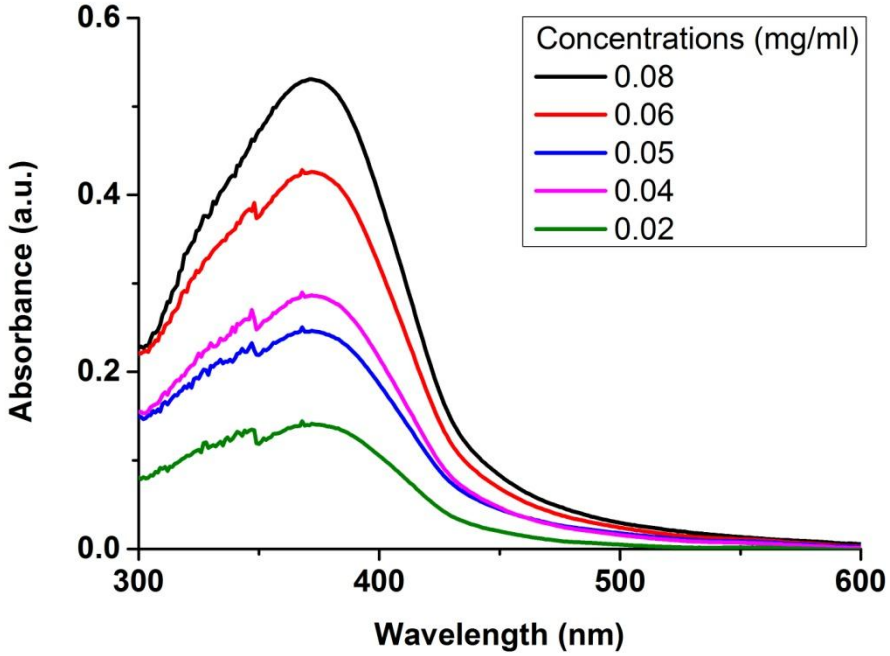

Figure A.3 P1 UV absorbance series for Molar absorptivity.

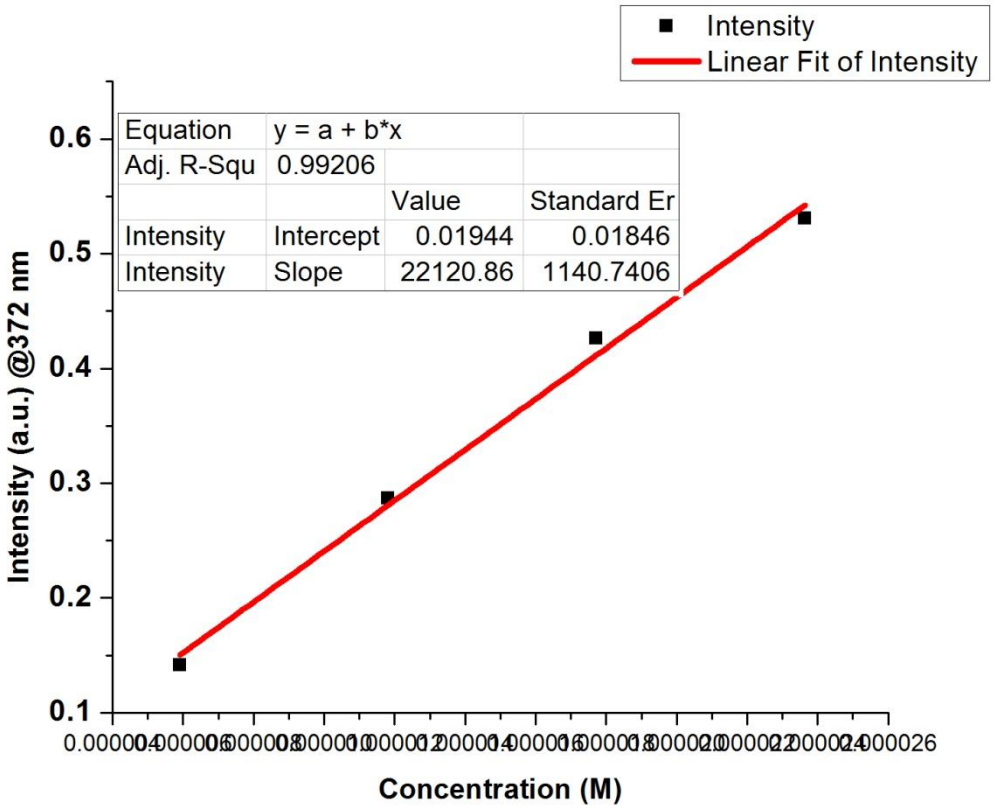

Figure A.4 P1 molar absorptivity in water.

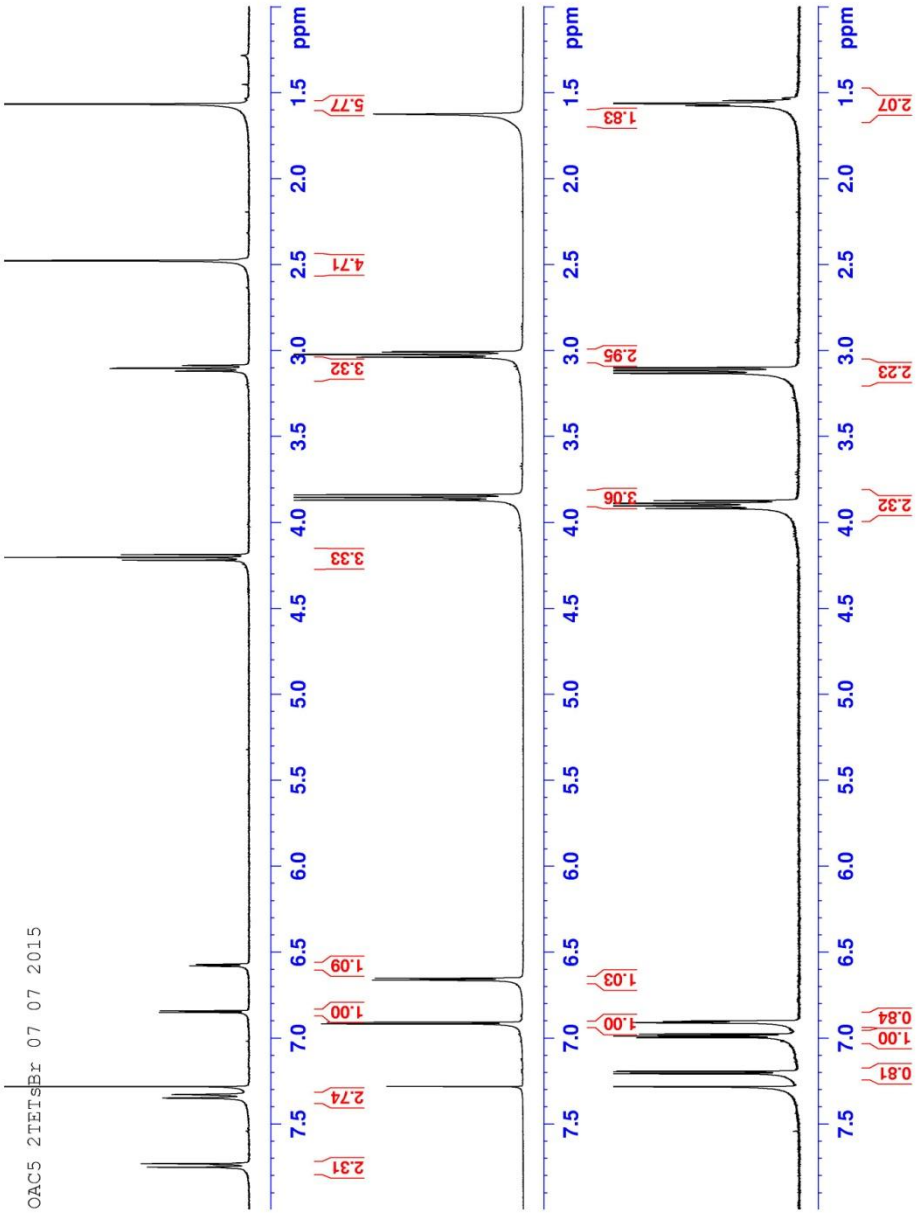

Figure A.5 ^{1}H-NMR overlay for M3 left, M1 middle and 2-(2-thienyl) ethanol right.

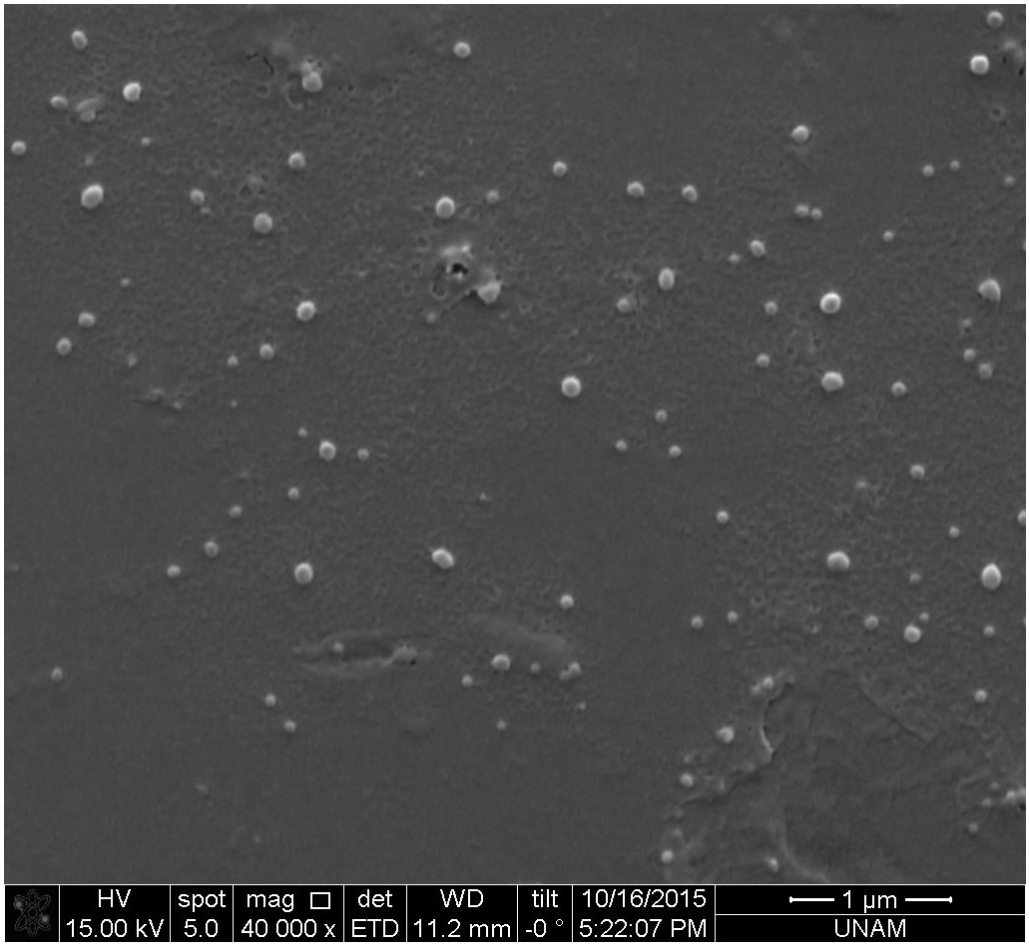

Figure A.6 P1 Self-assembled nanoparticles in water.

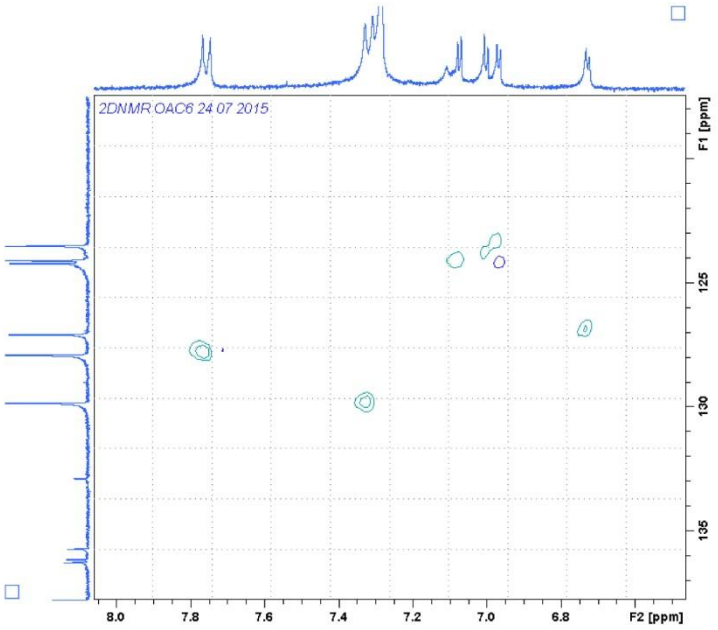

Figure A.7 TET2 2DNMR expanded aromatic region.

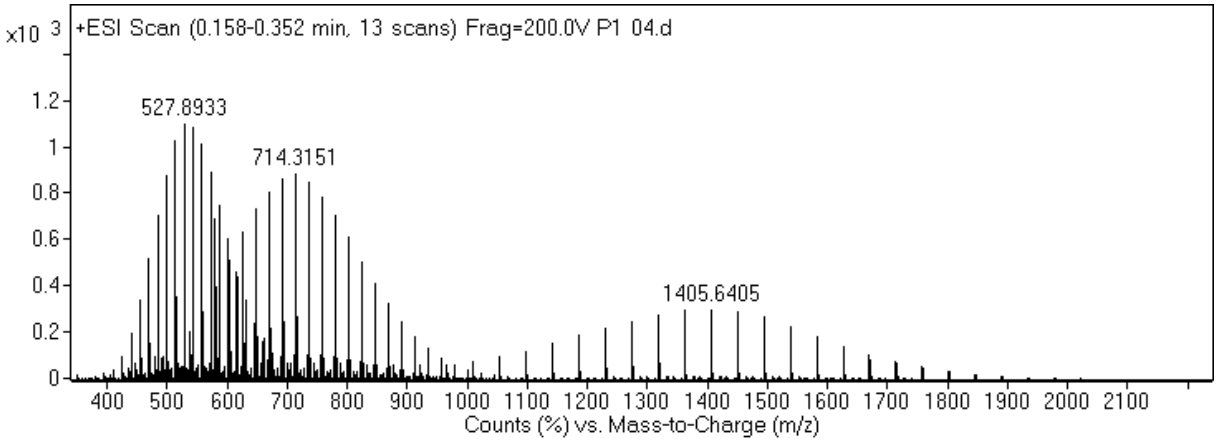

Figure A.8 Mass spectrum of P1 (positive mode)

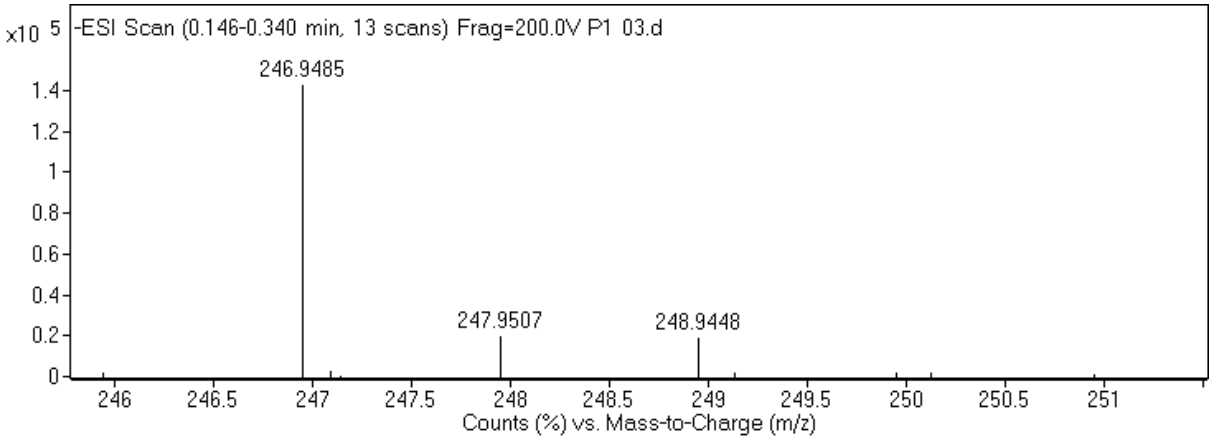

Figure A.9 Mass spectrum of P1 (negative mode)